Synthetic interleukin 22 (IL-22) signaling reveals biological activity of homodimeric IL-10 receptor 2 and functional cross-talk with the IL-6 receptor gp130

Received for publication, April 17, 2020, and in revised form, June 22, 2020 Published, Papers in Press, July 1, 2020, DOI 10.1074/jbc.RA120.013927

Sofie Mossner[1,‡], Marcus Kuchner[1,‡], Nastaran Fazel Modares[1], Birgit Knebel[2], Hadi Al-Hasani[2], Doreen M. Floss[1], and Jürgen Scheller[1,*]

From the [1]Institute of Biochemistry and Molecular Biology II and the [2]Institute for Clinical Biochemistry and Pathobiochemistry, German Diabetes Center, Medical Faculty, Heinrich-Heine-University, Düsseldorf, Germany

Edited by Ronald C. Wek

Cytokine signaling is transmitted by cell-surface receptors that function as biological switches controlling mainly immune-related processes. Recently, we have designed synthetic cytokine receptors (SyCyRs) consisting of GFP and mCherry nanobodies fused to transmembrane and intracellular domains of cytokine receptors that phenocopy cytokine signaling induced by non-physiological homo- and heterodimeric GFP-mCherry ligands. Interleukin 22 (IL-22) signals via both IL-22 receptor α1 (IL-22Rα1) and the common IL-10R2, belongs to the IL-10 cytokine family, and is critically involved in tissue regeneration. Here, IL-22 SyCyRs phenocopied native IL-22 signal transduction, indicated by induction of cytokine-dependent cellular proliferation, signal transduction, and transcriptome analysis. Whereas homodimeric IL-22Rα1 SyCyRs failed to activate signaling, homodimerization of the second IL-22 signaling chain, SyCyR (IL-10R2), which previously was considered not to induce signal transduction, led to induction of signal transduction. Interestingly, the SyCyR(IL-10R2) and SyCyR(IL-22Rα1) constructs could form functional heterodimeric receptor signaling complexes with the synthetic IL-6 receptor chain SyCyR(gp130). In summary, we have demonstrated that IL-22 signaling can be phenocopied by synthetic cytokine receptors, identified a functional IL-10R2 homodimeric receptor complex, and uncovered broad receptor cross-talk of IL-22Rα1 and IL-20R2 with gp130.

Cytokines control immune responses but are also involved in homeostatic processes, such as development, differentiation, growth, and regeneration. Signal transduction of cytokines is executed by natural biological switches, and among many other functions, it controls immunity-related processes (1). Cytokines switch transmembrane receptors from the off-state into the on-state via receptor dimerization or multimerization. The on-state might be interrupted by negative feedback mechanisms or depletion of the cytokine and cytokine receptor. Recently, we have designed synthetic cytokine receptors (SyCyRs), which phenocopy IL-6 and IL-23 signaling (2). SyCyRs are based on nanobodies specifically recognizing GFP and mCherry (3, 4) fused to the transmembrane and intracellular domains of the receptor of interest. The nanobodies serve as extracellular sensors for homo- and heteromeric GFP-mCherry fusion proteins, which induce receptor dimerization (5). A nanobody or VHH domain consists of the N-terminal variable domain of Camelidae heavy chain antibody, which is sufficient for antigen binding (6). Synthetic cytokine receptors might become important tools for immunotherapeutic applications (7), with chimeric antigen receptor (CAR) T-cell therapy being the first example that has been approved as gene therapy for the treatment of severe cases of acute lymphatic leukemia (8).

Moreover, synthetic cytokine biology can decipher the potential of cytokine receptor cross-talk. In a reductionistic view, a cytokine binds only to its corresponding cytokine receptor complex, which is composed either of receptor homo- or heterodimers. This simple view has been challenged for many cytokines and cytokine receptors that have multiple binding partners. For example, the signal receptor complex of IL-6 consists of two gp130 receptor chains, but gp130 is also the only receptor for IL-11 and the co-receptor for IL-27, CNTF, CT-1, LIF, and OSM. On the other hand, IL-35 from the IL-12–type cytokine family was proposed to activate a variety of different receptor complexes, including gp130 homodimers, IL-12Rβ2 homodimers, and IL-12Rβ2/WSX-1 and gp130/IL-12Rβ2 heterodimers (9, 10). Using chimeric cytokine receptors, we have shown that gp130 can form biologically active complexes with IL-23R, IL-12Rβ2, and IL-12Rβ1 of the closely related IL-12-type cytokine family (11). The Interleukin 10 family consists of six members, with IL-10, IL-22, and IL-26 belonging to the IL-10 family and IL-24, IL-20, and IL-19 belonging to the IL-20 subfamily (12, 13). There are three more distantly related cytokines that are sometimes classified as IL-10 family members or as type III interferons (IFNs): IL-28A (IFN-λ2), IL-28B (IFN-λ3), and IL-20 (IFN-λ1) (14). IL-22 signals via the IL-10R2 and IL-22Rα1 and mainly by activation of Jak-mediated STAT3 phosphorylation and, albeit to a lesser extent, also STAT1, STAT5, and ERK. Jak1 and Tyk2 are preferentially used by IL-10R2 and IL-22Rα1 (15, 16). IL-22 is predominantly produced by T-cell subsets and group 3 innate lymphoid cells (ILC3s) (17). In the intestinal epithelium, IL-22 is mainly responsible for immune homeostasis as well as wound healing (18) and plays important roles in the pathogenesis of many intestinal diseases. The majority of preclinical studies support a protective role for IL-22 against various pathogens, including bacteria, yeasts, viruses, and parasites (12). Therefore, mimicking IL-22

This article contains supporting information.
‡These authors contributed equally to this work.
*For correspondence: Jürgen Scheller, jscheller@uni-duesseldorf.de.

signal transduction in synthetic biology is of importance for future therapeutic applications. Here, we generated and characterized synthetic cytokine receptors for IL-22, revealed a novel role of the IL-10R2 in signal transduction, and found a functional cross-talk with the IL-6 receptor chain gp130.

Results

Synthetic cytokine receptors for IL-22 are biologically active and phenocopy natural IL-22 signaling

Here, we generated SyCyRs to mimic IL-22 signaling. Naturally, IL-22 signals via a heterodimer of IL-10R2 and IL-22Rα1. Whereas IL-22Rα1 is rather specific for IL-22, IL-20, and IL-24, IL-10R2 is shared with more cytokines of the IL-10 superfamily, including IL-10, IL-22, IL-26, and type III interferons: IL-28A/B and IL-29 (19–21). First, the mCherry-nanobody (C_{VHH}) was genetically fused to the transmembrane and intracellular domain of IL-10R2 in C_{VHH}IL-10R2 (Fig. 1*A* and Fig. S1*A*) and introduced into Ba/F3/gp130 cells. The transmembrane domain of the IL-22Rα1 was genetically fused to the GFP nanobody (G_{VHH}), resulting in G_{VHH}IL-22Rα1 (Fig. 1*A* and Fig. S1*A*). Expression of IL-22Rα1 and IL-10R2 in Ba/F3/gp130/IL-22Rα1/IL-10R2 cells or N-terminally HA-tagged C_{VHH}IL-10R2 and Myc-tagged GFP_{VHH}IL-22Rα1 in Ba/F3/gp130/C_{VHH}IL-10R2/G_{VHH}IL-22Rα1 cells was verified by flow cytometry (Fig. S1*B*). Ba/F3/gp130 cells are commonly used in cytokine research, because after activation of gp130 signaling by stimulation with, for example, Hyper-IL-6 (a fusion protein of IL-6 and the soluble IL-6R) (22), these cells proliferate following STAT3 and ERK activation (Fig. 1*B*). As expected, Hyper-IL-6 and IL-22 induced proliferation of Ba/F3/gp130/IL-10R2/IL-22Rα1 cells, whereas IL-22 and IL-22-Fc were not able to induce proliferation of Ba/F3/gp130/IL-10R2 cells. The pan-JAK inhibitor P6 generally blocked cytokine-induced proliferation of Ba/F3/gp130 cells and variants thereof (Fig. 1*B*). We have compared 10 and 100 μM P6, because both concentrations were used previously (23, 24). Here we decided to use the lower concentration because it was enough to inhibit proliferation of Ba/F3-gp130 cells (Fig. 1*B*), albeit the higher concentration resulted in a more profound inhibition of all analyzed Janus kinases (Fig. S1*C*). Among the tested synthetic ligands composed of homo- and heterodimeric GFP-mCherry fusion proteins, the heterodimeric GFP-mCherry induced proliferation of Ba/F3/gp130/C_{VHH}IL-10R2/G_{VHH}IL-22Rα1 cells but not of Ba/F3/gp130 cells, which was also inhibited by P6 (Fig. 1*C*). As a control, cells were also stimulated with monomeric GFP and mCherry, which did not induce cellular proliferation (Fig. 1*C*). For the stimulation with homodimeric GFP or mCherry, they were genetically fused to a cDNA coding for a human Fc tag, which facilitated homodimerization of GFP-Fc and mCherry-Fc (5). Whereas GFP-Fc also did not induce cellular proliferation, homodimeric mCherry-Fc induced cellular proliferation of Ba/F3/gp130/C_{VHH}IL-10R2/G_{VHH}IL-22Rα1 cells, suggesting that a synthetic dimer of C_{VHH}IL-10R2 but not of G_{VHH}IL-22Rα1 was biologically active (Fig. 1*C*). Fig. 1*D* showed that the proliferation rate of Ba/F3/gp130/C_{VHH}IL-10R2/G_{VHH}IL-22Rα1 and Ba/F3/gp130/IL-10R2/IL-22Rα1 cells depended on the concentration of the synthetic GFP-mCherry fusion protein or IL-22-Fc reaching the half-maximal proliferation at 5.5 ng/ml for GFP-mCherry and 2.1 ng/ml for IL-22-Fc, whereas GFP-mCherry failed to induce proliferation of Ba/F3/gp130/IL-10R2/IL-22Rα1 cells. We also performed this experiment with Ba/F3/gp130/G_{VHH}IL-10R2/C_{VHH}IL-22Rα1 cells, where the extracellular domains of the SyCyRs were reciprocally exchanged, and obtained similar results (Fig. S1*D*). Dimeric IL-22Fc selectively induced cellular proliferation via the IL-22Rα1/IL-10R2 heterodimer and did not induce proliferation of Ba/F3/gp130/IL-10R2 and Ba/F3/gp130/IL-22Rα1 cells (Fig. 1*E*).

IL-22 signals mainly via phosphorylated STAT3 and ERK1/2 induced via Jak1 and Tyk2 phosphorylation as shown in Ba/F3/gp130/IL-10R2/IL-22Rα1 cells, all of which could be inhibited by the P6 inhibitor at least to some extent, with the exception of Tyk2 (Fig. 2*A*) (25). P6 should inhibit all human Jaks (26); however, we observed a clear selectivity toward the preferential inhibition of murine Jak1, which might be also due to different inhibitory, capacity depending on the receptor composition. However, higher concentrations of P6 (100 μM) resulted in inhibition of all JAKs (Fig. S1*C*). Consequently, stimulation of Ba/F3/gp130/C_{VHH}IL-10R2/G_{VHH}IL-22Rα1 cells with GFP-mCherry induced phosphorylation of STAT3 and ERK1/2 as shown by Western blotting (Fig. 2*B*). As control, Hyper-IL-6 also induced pSTAT3 and pERK1/2 in Ba/F3/gp130/C_{VHH}IL-10R2/G_{VHH}IL-22Rα1 cells (Fig. 2*B*). Importantly, dimeric mCherry-Fc but not GFP-Fc also induced sustained phosphorylation of STAT3, ERK1/2, Jak1, and Tyk2 but also additionally of Jak2, which was not observed for natural and synthetic IL-22 signaling (Fig. 2, *A* and *B*). The phosphorylation of Tyk2 for human IL-10R2 homodimers has been shown previously (27). P6 suppressed STAT3, ERK1/2, and Jak1 phosphorylation, but not Jak2 and Tyk2 (Fig. 2*B*), suggesting that Jak1 is critical for synthetic cytokine receptor activation, which is also in agreement with natural IL-22 signaling (15, 16) (Fig. 2*A*).

Next, Ba/F3/gp130/IL-10R2/IL-22Rα1 and Ba/F3/gp130/G_{VHH}IL-10R2/C_{VHH}IL-22Rα1 cells were stimulated with IL-22-Fc and GFP-mCherry, respectively, for up to 480 min and STAT3 phosphorylation, and expression of SOCS3 was monitored by Western blotting. IL-22-Fc and GFP-mCherry induced STAT3 phosphorylation within 5–10 min of cellular stimulation, which was slightly down-regulated after 480 min only in Ba/F3 cells expressing the suitable natural or synthetic receptor combination (Fig. 2*C*). SOCS3 is a target gene of STAT3 and is up-regulated after IL-22-Fc and GFP-mCherry stimulation of Ba/F3/gp130/IL-10R2/IL-22Rα1 and Ba/F3/gp130/G_{VHH}IL-10R2/C_{VHH}IL-22Rα1 cells, respectively, after about 60–120 min of stimulation (Fig. 2*C*), whereas no SOCS3 expression was observed in Ba/F3/gp130/IL-10R2/IL-22Rα1 cells stimulated with GFP-mCherry and Ba/F3/gp130/C_{VHH}IL-10R2/G_{VHH}IL-22Rα1 cells stimulated with IL-22-Fc.

Further, we analyzed the mRNA expression by gene array analysis of Ba/F3/gp130/IL-10R2/IL-22Rα1 cells stimulated with IL-22 and Ba/F3/gp130/C_{VHH}IL-10R2/G_{VHH}IL-22Rα1 cells stimulated with GFP-mCherry, indicating a high overlap of gene regulation. In Fig. 3*A*, all conditions were compared between the different cell lines in one scattered blot, which revealed a high degree of overlap. In Fig. 3 (*B* and *C*), we

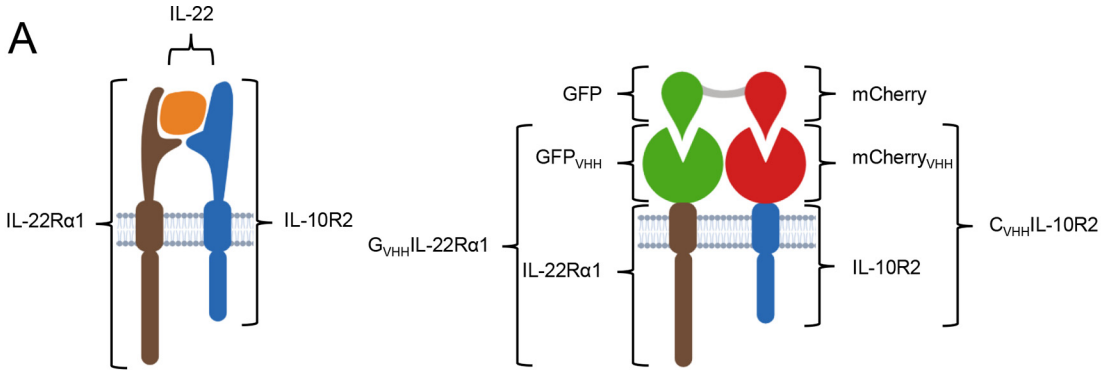
A
IL-22
IL-22Rα1
IL-10R2
GVHHIL-22Rα1
GFP
GFPVHH
IL-22Rα1
mCherry
mCherryVHH
IL-10R2
CVHHIL-10R2

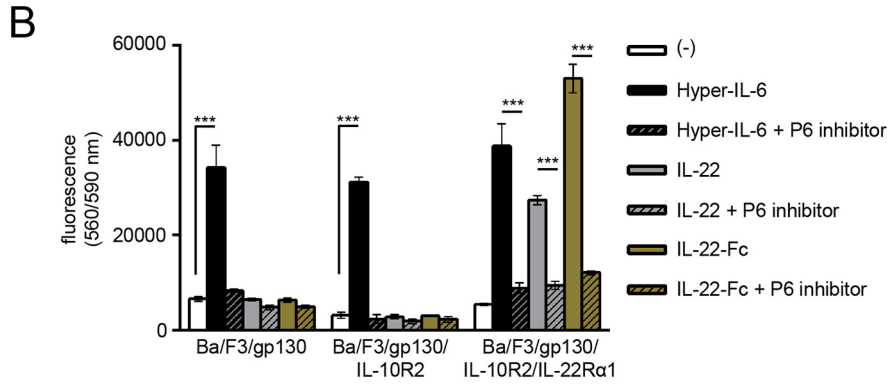
B
fluorescence (560/590 nm)
60000
40000
20000
0
***
Ba/F3/gp130
Ba/F3/gp130/ IL-10R2
Ba/F3/gp130/ IL-10R2/IL-22Rα1
(-)
Hyper-IL-6
Hyper-IL-6 + P6 inhibitor
IL-22
IL-22 + P6 inhibitor
IL-22-Fc
IL-22-Fc + P6 inhibitor

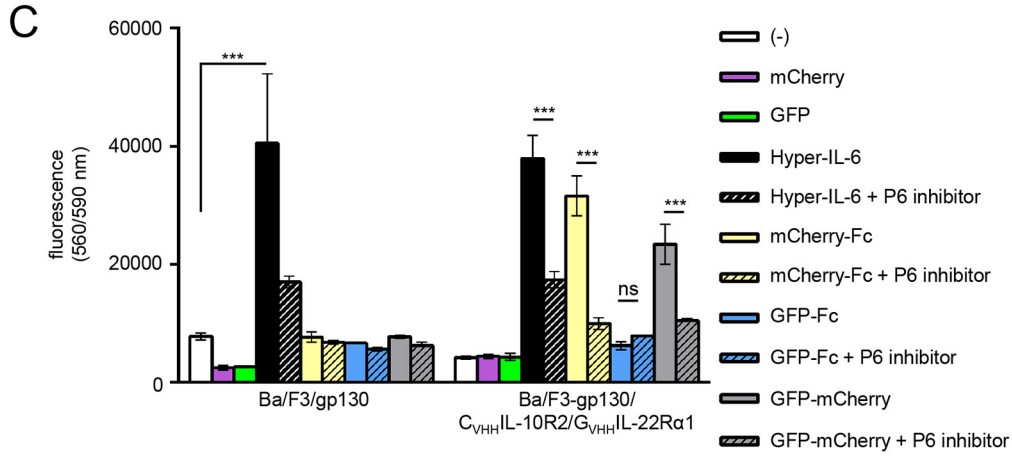
C
fluorescence (560/590 nm)
60000
40000
20000
0
***
ns
Ba/F3/gp130
Ba/F3-gp130/ CVHHIL-10R2/GVHHIL-22Rα1
(-)
mCherry
GFP
Hyper-IL-6
Hyper-IL-6 + P6 inhibitor
mCherry-Fc
mCherry-Fc + P6 inhibitor
GFP-Fc
GFP-Fc + P6 inhibitor
GFP-mCherry
GFP-mCherry + P6 inhibitor

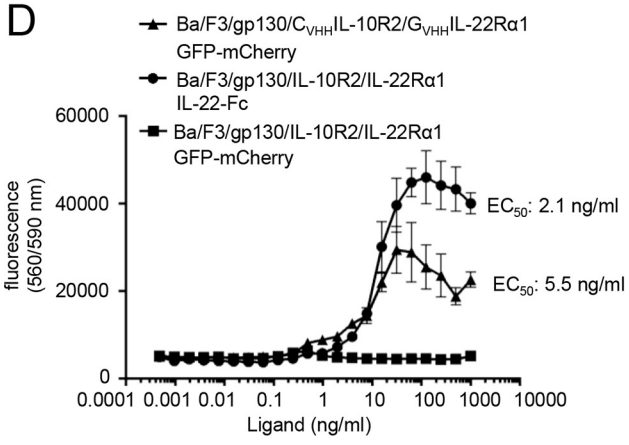
D
Ba/F3/gp130/CVHHIL-10R2/GVHHIL-22Rα1 GFP-mCherry
Ba/F3/gp130/IL-10R2/IL-22Rα1 IL-22-Fc
Ba/F3/gp130/IL-10R2/IL-22Rα1 GFP-mCherry
fluorescence (560/590 nm)
60000
40000
20000
0
EC50: 2.1 ng/ml
EC50: 5.5 ng/ml
0.0001 0.001 0.01 0.1 1 10 100 1000 10000
Ligand (ng/ml)

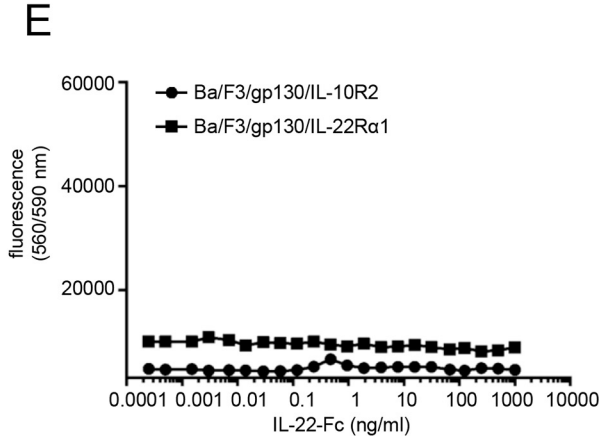
E
Ba/F3/gp130/IL-10R2
Ba/F3/gp130/IL-22Rα1
fluorescence (560/590 nm)
60000
40000
20000
0.0001 0.001 0.01 0.1 1 10 100 1000 10000
IL-22-Fc (ng/ml)

specifically compared unstimulated and stimulated conditions of one cell line and observed an activation of gene transcription upon stimulation that was stronger for IL-22 compared with the GFP-mCherry stimulated cell line. However, among the regulated genes are, in both conditions, typical STAT3 target genes, including SOCS3, Pim-1, and Myc (Fig. 3*D*). mRNA level of SOCS3, Pim-1, and Myc was verified by qPCR (Fig. 4), supporting our data obtained from the gene array analysis. In summary, our data revealed a high degree of overlap between the signaling induced by the synthetic ligand GFP-mCherry and the natural cytokine IL-22.

SyCyRs for IL-22Rα1 fail to form biologically active homodimers

Next, we used Ba/F3/gp130/G_{VHH}IL-22Rα1 cells (Fig. S2*A*) to verify that homodimers of the synthetic IL-22Rα1 are not biologically active as suggested in Fig. 1*C*. Cell-surface expression of G_{VHH}IL-22Rα1 was verified by flow cytometry (Fig. S2*B*). Dimeric GFP-Fc was not able to induce cellular proliferation of Ba/F3/gp130 and Ba/F3/gp130/G_{VHH}IL-22Rα1 cells (Fig. S2*C*). Also, monomeric and dimeric GFP-Fc did not induce STAT3 and ERK1/2 phosphorylation (Fig. S2*D*). As a control, Hyper-IL-6 induced cellular proliferation and STAT3 and ERK1/2 phosphorylation (Fig. S2, *C* and *D*). We also performed this experiment with Ba/F3/gp130/C_{VHH}IL-22Rα1 cells and dimeric mCherry and obtained comparable results (Fig. S3, *A* and *B*). Interestingly, the overall assembly of G_{VHH}IL-22Rα1 was correct because we showed binding of GFP-Fc to Ba/F3/gp130/G_{VHH}IL-22Rα1 but not to Ba/F3/gp130 cells by flow cytometry (Fig. S3*C*). In conclusion, SyCyRs for IL-22Rα1 fail to form biologically active homodimers. This finding was surprising because the intracellular domain of the long-chain cytokine receptor IL-22Rα1 is 346 amino acid residues long, and apart from binding sites for Jak1, it also contains multiple initiation sites for signal transduction (*e.g.* STATs) (25).

SyCyRs for IL-10R2 form biologically active homodimers

Receptors with short ICDs including IL-10R2 often bind their ligands with lower affinity, pair with Tyk2 or Jak2 (27), and are generally considered to minimally contribute to STAT recruitment and activation (28, 29). Only in combination with long-chain receptors, such as IL-22Rα1, do this kind of receptors contribute to activation of signal transduction. On the other hand, results presented in Figs. 1 and 2 suggest that homodimers of IL-10R2 induce signal transduction that is highly similar to signaling induced by IL-10R2/IL-22Rα1 heterodimers. In line with this, Kotenko *et al.* (27) already showed that a chimeric homodimer of human IL-10R2 is able to phosphorylate STAT1. Therefore, we generated Ba/F3/gp130/C_{VHH}IL-10R2 cells (Fig. 5*A*). Cell-surface expression of C_{VHH}IL-10R2 was verified by flow cytometry (Fig. S4*A*). The proliferation of Ba/F3/gp130/C_{VHH}IL-10R2 cells depended on the concentration of synthetic mCherry-Fc fusion proteins, reaching the half-maximal proliferation at 41.74 ng/ml (Fig. 5*B*). mCherry-Fc–induced proliferation of Ba/F3/gp130/C_{VHH}IL-10R2 cells was inhibited by P6 (Fig. 5*C*). Western blotting of Ba/F3/gp130/C_{VHH}IL-10R2 cells showed that mCherry-Fc induced STAT3, ERK1/2, Jak1, Jak2, and Tyk2 phosphorylation, whereas monomeric mCherry was not able to induce signal transduction (Fig. 5*D*). P6 selectively inhibited phosphorylation of Jak1 but not of Jak2 and Tyk2 and resulted in STAT3 suppression and ERK1/2 phosphorylation (Fig. 5*D*). The inhibition of Jak2 and Tyk2 phosphorylation was achieved using higher concentrations of 100 μM P6 (Fig. S1*C*). The IL-10R2 was also able to phosphorylate STAT3 when expressed with a GFP_{VHH}, resulting in Ba/F3/gp130/G_{VHH}IL-10R2 cells (Fig. S4*B*). The finding that C_{VHH}IL-10R2 homodimerization induced activation of Jak1, Jak2, and Tyk2 was supported by co-immunoprecipitation experiments using transiently transfected HEK293T cells. Here, precipitation of Jak1, Jak2, and Tyk2 resulted in co-immunoprecipitation of G_{VHH}IL-10R2, suggesting that all three tyrosine kinases are physically interacting with the intracellular domain of G_{VHH}IL-10R2 (Fig. 5*E*).

Next, we analyzed the mRNA expression by gene array analysis of Ba/F3/gp130/C_{VHH}IL-10R2/G_{VHH}IL-22Rα1 cells stimulated either with GFP-mCherry or mCherry-Fc, indicating a high overlap of gene regulation (Fig. 6*A*). In Fig. 6 (*B* and *C*), we specifically compared unstimulated and stimulated conditions either as homo- or heterodimer of the cell line and observed an activation of gene transcription upon stimulation that was comparable between the synthetic cytokine stimulations. However, among the regulated genes are, in both conditions, typical STAT3 target genes, including SOCS3, Pim-1, and Myc (Fig. 6*D*). mRNA level of SOCS3, Pim-1, and Myc was verified by qPCR (Fig. 6*E*), supporting our data obtained from the gene array analysis. This indicates that the IL-10R2 homodimer can induce nearly the same signal transduction as the IL-10R2/IL-22Rα1 heterodimer.

Deletions within the intracellular domain of the IL-10R2 abrogate signaling

In the intracellular domain of the IL-10R2, no obvious Janus kinase–binding sites, such as the typical box 1 and box 2 motifs, and no canonical tyrosine-dependent phosphorylation motifs

Figure 1. Stimulation of IL-22 signaling via synthetic G_{VHH}IL-22-Rα1 and C_{VHH}IL-10R2 cytokine receptors and WT signaling using Ba/F3/gp130/IL-10R2/IL-22Rα1 cells. *A*, schematic illustration of IL-22 (*orange*) binding to the IL-10R2 (*brown*) and the IL-22Rα1 (*blue*) to induce signal transduction. Also shown is synthetic GFP-mCherry (*green*, *red*) fusion protein binding to G_{VHH}IL-22Rα1 (*green*, *brown*) and C_{VHH}IL-10R2 (*red*, *blue*) and thereby mimicking the IL-22 signal transduction. This image was created with BioRender. *B*, proliferation of Ba/F3/gp130, Ba/F3/gp130/IL-10R2 and Ba/F3/gp130/IL-10R2/IL-22Rα1 cells without cytokine (−), with 10 ng/ml Hyper-IL-6, 100 ng/ml IL-22 or IL-22-Fc. 10 μM P6 inhibitor was added to the indicated conditions. *Error bars*, S.D. ***, $p < 0.001$. One representative experiment, with three biological replicates, of four is shown. *C*, proliferation of Ba/F3/gp130 and Ba/F3/gp130/C_{VHH}IL-10R2/G_{VHH}IL-22Rα1 cells without cytokine (−), in the presence of 10 ng/ml Hyper-IL-6 or in the presence of 100 ng/ml mCherry, GFP, mCherry-Fc, GFP-FC, GFP-mCherry. 10 μM P6 inhibitor was added to the indicated conditions. *Error bars*, S.D. ***, $p < 0.001$; *ns*, not significant. One representative experiment, with three biological replicates, of four is shown. *D*, proliferation of Ba/F3/gp130/IL-10R2/IL-22Rα1 cells incubated with increasing concentrations of IL-22-Fc and GFP-mCherry and Ba/F3/gp130/C_{VHH}IL-10R2/G_{VHH}IL-22Rα1 cells incubated with increasing concentrations of GFP-mCherry from 0.0001 to 1000 ng/ml. *Error bars*, S.D. One representative experiment, with four biological replicates, of three is shown. *E*, proliferation of Ba/F3/gp130/IL-10R2 and Ba/F3/gp130/IL-22Rα1 cells with increasing concentrations of IL-22-Fc from 0.0001 to 1000 ng/ml. *Error bars*, S.D. One representative experiment, with four biological, replicates, of three is shown.

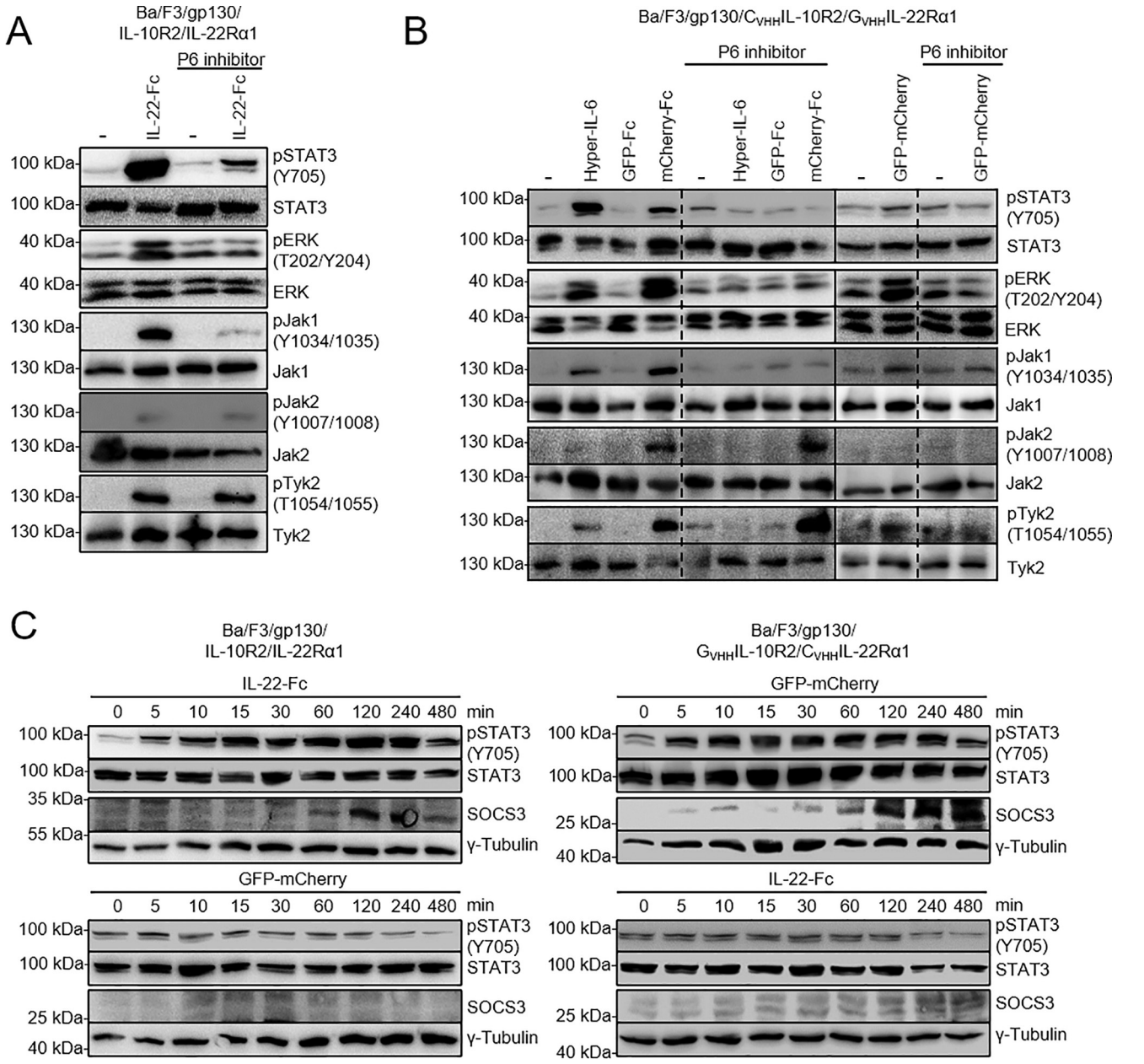

Figure 2. Stimulation of WT and synthetic IL-22 signaling analyzed by Western blotting. *A*, STAT3, ERK1/2, Jak1, Jak2, and Tyk2 activation of Ba/F3/gp130/IL-10R2/IL-22Rα1 cells treated with 100 ng/ml IL-22 for 120 min. Cells treated with P6 inhibitor were preincubated with 10 μM P6 for 30 min and then stimulated for 120 min. Equal amounts of proteins (50 μg/lane) were analyzed via specific antibodies detecting phospho-STAT3, -ERK1/2, -Jak1, -Jak2, and -Tyk2 and STAT3, ERK1/2, Jak1, Jak2, and Tyk2. Western blotting data show one representative experiment of three. *B*, STAT3, ERK1/2, Jak1, Jak2, and Tyk2 activation in Ba/F3/gp130/C$_{VHH}$IL-10R2/G$_{VHH}$IL-22Rα1 cells treated with 10 ng/ml Hyper-IL-6 or 100 ng/ml GFP-Fc, mCherry-Fc, GFP-mCherry for 120 min. Cells treated with the P6 inhibitor were preincubated with 10 μM P6 for 30 min and then also stimulated for 120 min. Equal amounts of protein (50 μg/lane) were analyzed via specific antibodies detecting phospho-STAT3, -ERK1/2, -Jak1, -Jak2, and -Tyk2 and STAT3, ERK1/2, Jak1, Jak2, and Tyk2. *Vertical lines* indicate different membranes, whereas *dashed lines* indicate cutting of the same membrane. Western blotting data show one representative experiment of three. *C*, Ba/F3/gp130/IL-10R2/IL-22Rα1 and Ba/F3/gp130/C$_{VHH}$IL-10R2/G$_{VHH}$IL-22Rα1 cells were stimulated with 100 ng/ml IL-22 and GFP-mCherry for 0–480 min. Equal amounts of total protein (50 μg/lane) were loaded followed by immunoblotting using specific antibodies for phospho-STAT3 and STAT3, SOCS, and γ-tubulin. Western blotting data show one representative experiment of three.

are present. Additionally, the intracellular domain of the IL-10R2 contains only one tyrosine amino acid residue, which is directly located at the border of the transmembrane domain and is not imbedded in a STAT3 or ERK activation motif. To decipher signal transduction, we generated deletion variants of the intracellular domain of the C$_{VHH}$IL-10R2, with deletions after amino acid 255 (Δ255), 280 (Δ280), 310 (Δ310), and 330 (Δ330) (based on the WT sequence of IL-10R2) (Fig. 7*A* and Fig. S5*A*). Ba/F3/gp130 cells were generated expressing exclusively the C$_{VHH}$IL-10R2 or the respective deletion variant. Cell-surface expression was verified by flow cytometry (Fig. S5*B*). As control, all Ba/F3/gp130/C$_{VHH}$IL-10R2 cells proliferated in the presence of Hyper-IL-6. Again, Ba/F3/gp130/C$_{VHH}$IL-10R2 cells proliferated in the presence of mCherry-Fc. Of the deletion variants, only Ba/F3/gp130/C$_{VHH}$IL-10R2(Δ330) showed sustained proliferation, whereas all other deletion variants did

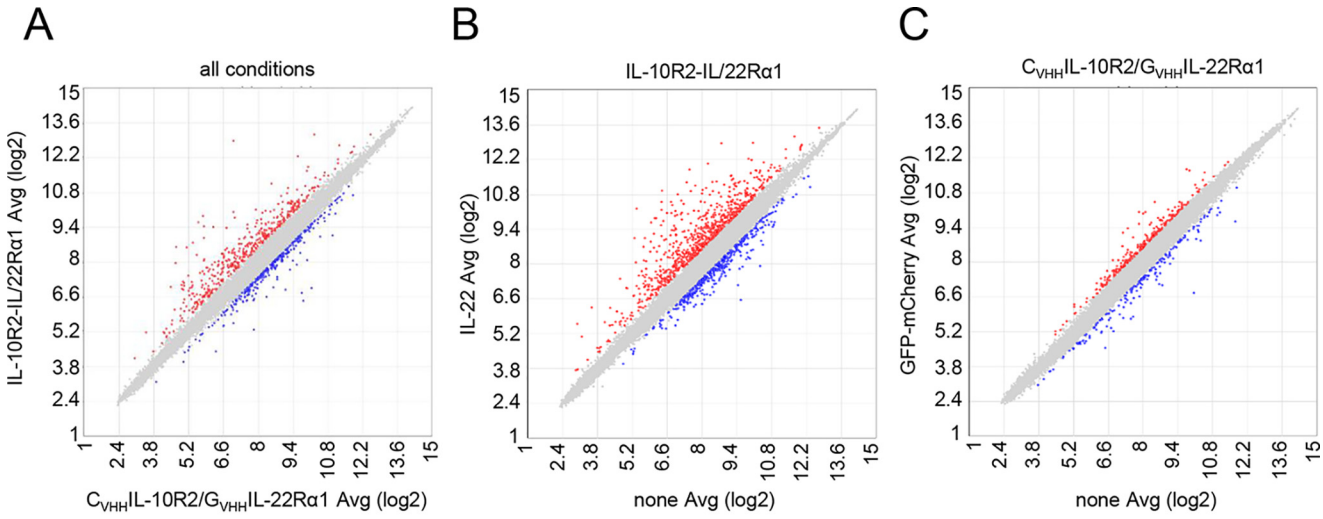

D

IL-22 vs. none		GFP-mCherry vs. none		Gene
Fold change	P-val	Fold change	P-val	
19.84	$3.84*10^{-20}$	1.88	$2.73*10^{-9}$	Socs3
15.05	$1.57*10^{-10}$	2.17	0.0004	IL-6
7.13	$1.39*10^{-6}$	3.87	0.0003	Ier3
5.15	$6.95*10^{-10}$	3.55	$2.52*10^{-8}$	Pim-1
3.22	$7.58*10^{-10}$	2.78	$1.27*10^{-9}$	Gpr84
2.94	$1.06*10^{-5}$	2.12	0.0015	Fas
1.72	$1.69*10^{-7}$	1.87	$2.65*10^{-8}$	Myc
1.61	0.0004	1.78	0.0003	Ifngr2
-5.35	$6.06*10^{-11}$	-1.54	0.0006	Mc5r
-3.38	$4.73*10^{-7}$	-1.58	0.0021	Sh2d3c
-1.54	0.0122	-1.61	0.0004	Gpx2

Figure 3. Microarray analysis of Ba/F3/gp130 cells expressing either the WT or synthetic receptors of IL-22Rα1 and IL-10R2. The comparison was performed with 1.5-fold. Varying up-regulated genes are shown in *red* and down-regulated genes in *blue*. *A*, scatter plot comparing mRNA levels of Ba/F3/gp130/IL-10R2/IL-22Rα1 and Ba/F3/gp130/C_{VHH}IL-10R2/G_{VHH}IL-22Rα1 cells stimulated for 120 min with either 100 ng/ml IL-22 or GFP-mCherry. *B*, scatter plot comparing mRNA levels of Ba/F3/gp130/IL-10R2/IL-22Rα1 cells either unstimulated or stimulated with IL-22 for 120 min. *C*, scatter plot comparing mRNA levels of Ba/F3/gp130/C_{VHH}IL 10R2/G_{VHH}IL 22Rα1 cells either unstimulated or stimulated with GFP-mCherry for 120 min. *D*, list of up- or down-regulated mRNAs for Ba/F3/gp130/IL-10R2/IL-22Rα1 and Ba/F3/gp130/C_{VHH}IL-10R2/G_{VHH}-IL-22Rα1 cells with respective -fold change and *p* value.

not facilitate cellular proliferation with 100 ng/ml mCherry-Fc (Fig. 7*B*). At this concentration of mCherry-Fc, homodimeric C_{VHH}IL-10R2(Δ330) but not C_{VHH}IL-10R2(Δ310) expression of Pim1 mRNA was induced as quantified by qPCR (Fig. 7*C*). The EC_{50} of Ba/F3/gp130/C_{VHH}IL-10R2(Δ330) cells was 54.78 ng/ml mCherry-Fc and comparable with the EC_{50} of Ba/F3/gp130/C_{VHH}IL-10R2 cells of 51.42 ng/ml mCherry-Fc in this experiment. Interestingly, also Ba/F3/gp130/C_{VHH}IL-10R2 (Δ310) slightly proliferated in the presence of mCherry-Fc, albeit at a much higher concentration and did not reach maximal proliferation at 1000 ng/ml mCherry-Fc (Fig. 7*D*). Next, we analyzed STAT3, ERK1/2, Jak1, Jak2, and Tyk2 phosphorylation of the C_{VHH}IL-10R2 deletion variants in Ba/F3 cells. As shown in Fig. 7*E*, C_{VHH}IL-10R2(Δ330) exhibited the previously detected phosphorylation pattern of C_{VHH}IL-10R2 stimulated with 100 ng/ml mCherry-Fc. Interestingly, also C_{VHH}IL-10R2 (Δ310) showed only some STAT3, Jak1, Jak2, and Tyk2 phosphorylation, whereas the activation of ERK1/2 was lost. Most likely this explains why activation of this receptor fails to induce cellular proliferation. Stimulation of C_{VHH}IL-10R2(Δ280) and C_{VHH}IL-10R2(Δ255) with mCherry-Fc did not result in activation of signal transduction due to defective Jak activation (Fig. 7*E*). These results suggest that the amino acid residues from 310 to 330 but not from 330 to the C terminus are critically needed for signal transduction of homodimeric C_{VHH}IL-10R2. Interestingly, slightly reduced Jak phosphorylation was observed for C_{VHH}IL-10R2(Δ330) and C_{VHH}IL-10R2(Δ310), whereas larger deletions within the C_{VHH}IL-10R2 result in

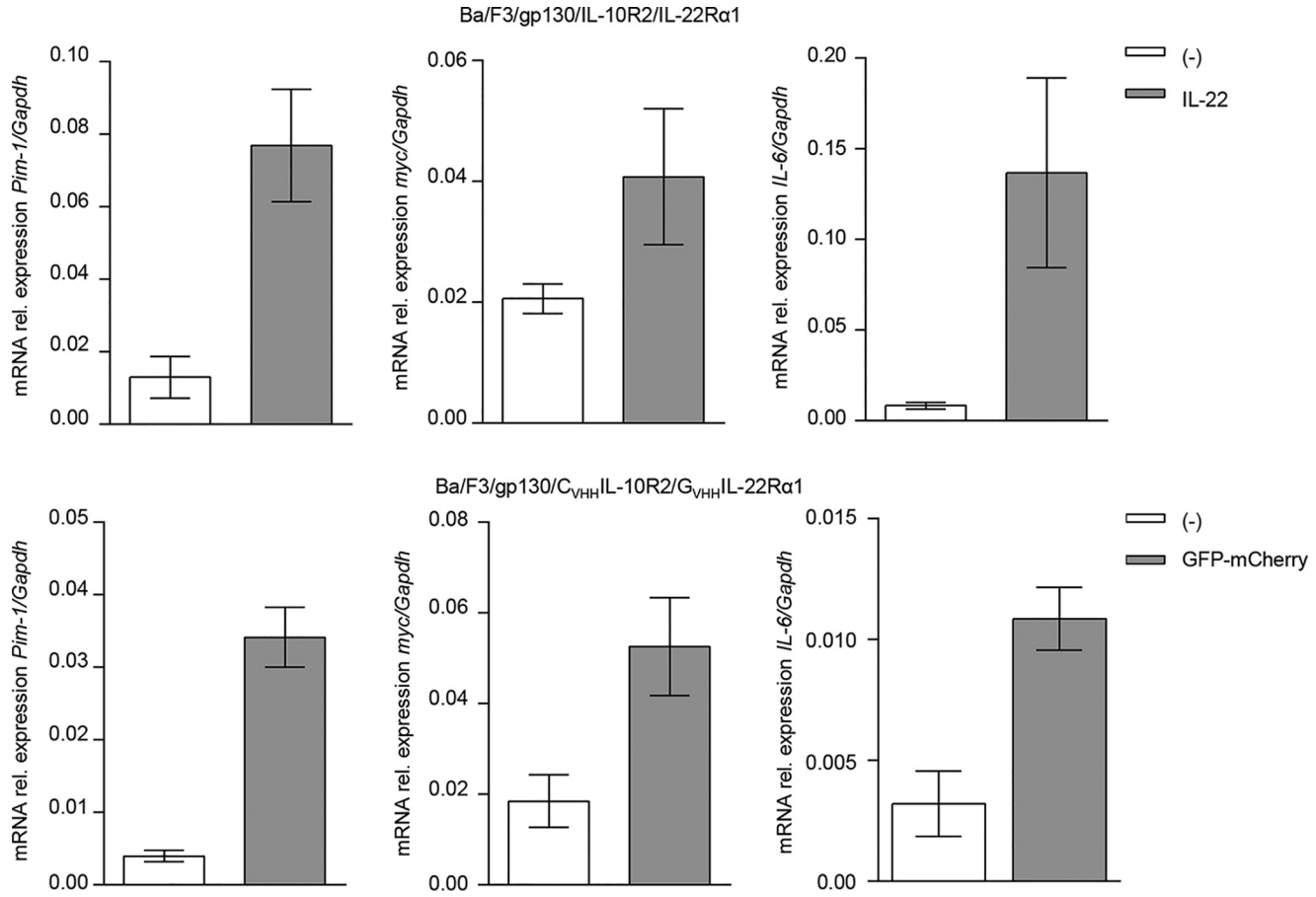

Figure 4. Verification of microarray data by quantification of mRNA expression of three genes (*Pim-1*, *IL-6*, and *myc*) for Ba/F3/gp130/IL-10R2/IL-22Rα1 and Ba/F3/gp130/C_{VHH}IL-10R2/G_{VHH}IL-22Rα1 cells. *Error bars*, S.D. One representative experiment, with three biological replicates, of four is shown.

complete abrogation of Jak phosphorylation, suggesting that the binding sites of Jak1, Jak2, and Tyk2 are mainly located between amino acid residues 280 and 310.

Amino acid exchanges of prolines 320 and 323 within the intracellular domain of the IL-10R2 only minimally reduce signaling capacity

We identified a putative P*XX*P motif within the intracellular domain of the IL-10R2, which might be involved in noncanonical induction of signal transduction (Fig. 8*A*) and mutated proline 320 and proline 323 into alanine (C_{VHH}IL-10R2(P320A, P323A), C_{VHH}IL-10R2(P320A,P323A,Δ330) (Fig. S6*A*) and generated stably transduced Ba/F3/gp130 cells (Fig. S6*B*). Proliferation of Ba/F3/gp130/C_{VHH}IL-10R2(P320A,P323A) and Ba/F3/gp130/C_{VHH}IL-10R2(P320A,P323A,Δ330) cells was, however, still induced by mCherry-Fc, albeit with a slightly higher EC_{50} of 73.2 and 71.2 ng/ml, respectively (Fig. 8, *B* and *C*), which was also reflected in the slightly reduced induction of the target gene Pim-1 as compared with WT IL-10R2 (Fig. 8*D*). Also signal transduction was only minimally affected by mutation of the two prolines, and if there was any, then STAT3 phosphorylation was slightly reduced (Fig. 8*E*). In conclusion, prolines 320 and 323 within the P*XX*P motif had no effect on signal transduction of homodimeric C_{VHH}IL-10R2.

SyCyRs for IL-10R2 and IL-22Rα1 form biologically active heterodimers with the IL-6 signal-transducing receptor chain gp130

Previously, we have generated SyCyRs for gp130, which is the main signaling receptor of IL-6 type cytokines. Homodimeric gp130 receptor complexes are induced by IL-6, IL-11, and IL-35, homodimeric SyCyRs for gp130 phenocopy IL-6 signaling *in vitro* and *in vivo* (2, 9). Here, we analyzed whether C_{VHH}gp130 can form functional heterodimeric complexes with G_{VHH}IL-10R2 (Fig. 9*A* and Fig. S7*A*). Both SyCyRs were expressed in stably transduced Ba/F3/gp130/G_{VHH}IL-10R2/C_{VHH}gp130 cells as shown by flow cytometry of Myc-tagged G_{VHH}IL-10R2 and HA-tagged C_{VHH}gp130 (Fig. S7*B*). GFP-mCherry induced sustained proliferation of Ba/F3/gp130/G_{VHH}IL-10R2/C_{VHH}gp130 cells via G_{VHH}IL-10R2/C_{VHH}gp130 heterodimeric receptor complex (Fig. 9*B*). Dimeric mCherry induced also proliferation of these cells via C_{VHH}gp130 homodimers as shown previously (Fig. 9*B*) (5). The EC_{50} of GFP-mCherry–induced proliferation of Ba/F3/gp130/G_{VHH}IL-10R2/C_{VHH}gp130 cells was 64 ng/ml (Fig. 9*C*). Thus, STAT3 and ERK1/2 phosphorylation was also specifically induced via G_{VHH}IL-10R2/C_{VHH}gp130 heterodimeric receptor complexes induced by GFP-mCherry and G_{VHH}IL-10R2 homodimeric receptor complexes induced by 2xGFP (Fig. 9*D*).

We also analyzed whether G_{VHH}gp130 can form functional heterodimeric complexes with C_{VHH}IL-10R2(Δ310) and C_{VHH}IL-10R2(Δ280) (Fig. 10*A*). Both SyCyRs were expressed in Ba/F3/gp130/G_{VHH}gp130/C_{VHH}IL-10R2(Δ280) and Ba/F3/gp130/G_{VHH}gp130/C_{VHH}IL-10R2(Δ310) cells as shown by flow cytometry of the Myc-tagged G_{VHH}gp130 and HA-tagged

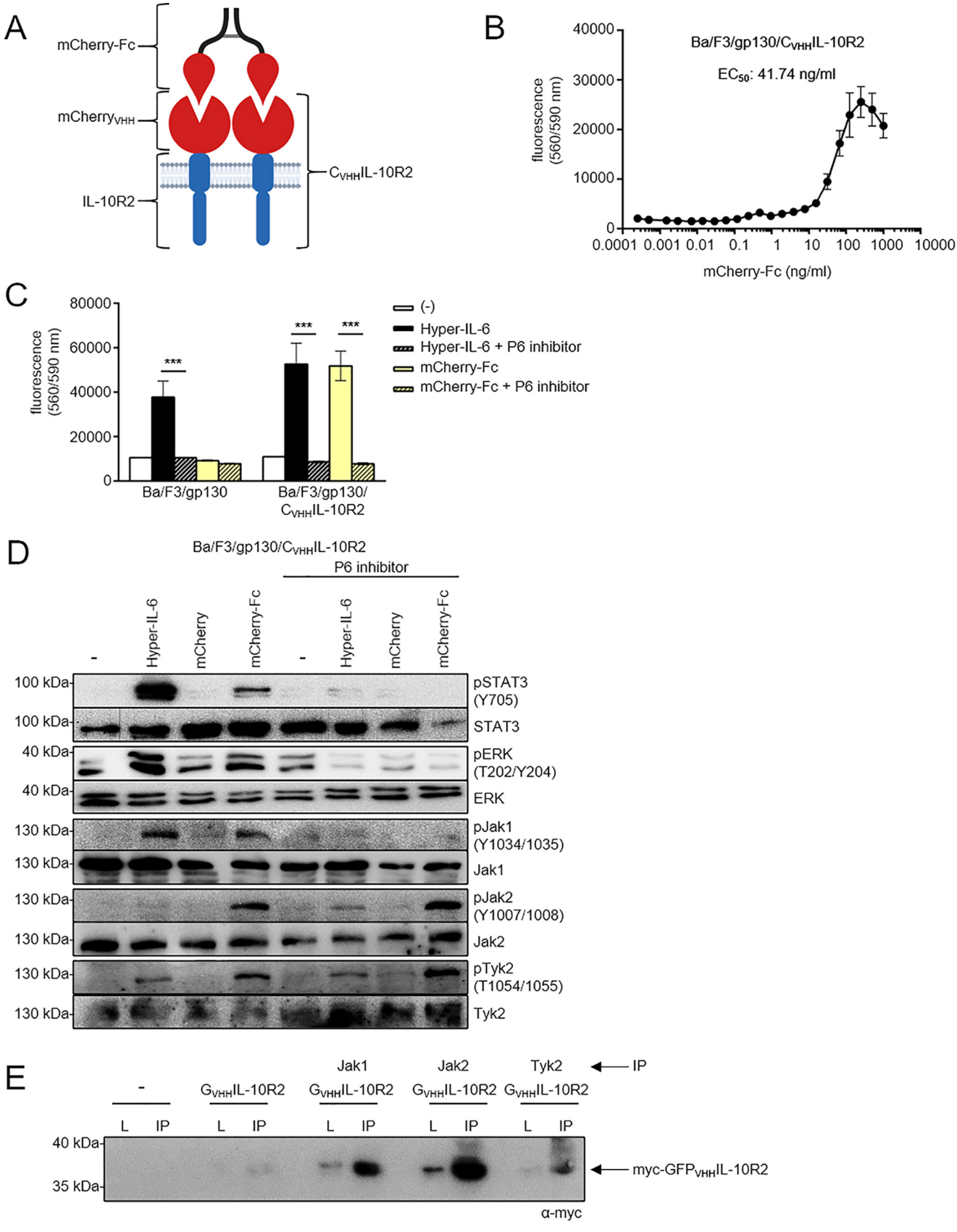

C_{VHH}IL-10R2 (Fig. S8). GFP-mCherry induced proliferation of Ba/F3/gp130/G_{VHH}gp130/C_{VHH}IL-10R2(Δ310) but not of Ba/F3/gp130/G_{VHH}gp130/C_{VHH}IL-10R2(Δ280) cells via the G_{VHH}gp130/C_{VHH}IL-10R2 heterodimeric receptor complexes (Fig. 10*B*). The EC_{50} of GFP-mCherry–induced proliferation of Ba/F3/gp130/G_{VHH}gp130/C_{VHH}IL-20R2(Δ310) cells was 7.8 ng/ml (Fig. 10*C*). Thus, STAT3 and ERK phosphorylation was also specifically induced via G_{VHH}gp130/C_{VHH}IL-10R2(Δ310) heterodimeric receptor complexes induced by GFP-mCherry (Fig. 10*D*) but not via G_{VHH}gp130/C_{VHH}IL-10R2(Δ280). This result suggests that the STAT3 and ERK phosphorylation is solely based on phosphorylation of the intracellular gp130 receptor chain in the gp130/IL-10R2Δ310 receptor complex, because we have previously shown that the IL-10R2Δ310 is not able to induce STAT3 and ERK activation but has residual JAK activity.

Finally, we also analyzed whether G_{VHH}gp130 can form functional heterodimeric complexes with C_{VHH}IL-22Rα1 (Fig. 11*A* and Fig. S9*A*). Both SyCyRs were expressed in Ba/F3/gp130/G_{VHH}gp130/C_{VHH}IL-22Rα1 cells as shown by flow cytometry of the Myc-tagged G_{VHH}gp130 and HA-tagged C_{VHH}IL-22Rα1 (Fig. S9*B*). GFP-mCherry induced proliferation of Ba/F3/gp130/G_{VHH}gp130/C_{VHH}IL-22Rα1 cells via the G_{VHH}gp130/C_{VHH}IL-22Rα1 heterodimeric receptor complex (Fig. 11*B*), whereas monomeric GFP or mCherry did not induce cellular proliferation (Fig. 11*B*). Also, dimeric GFP induced proliferation of these cells via G_{VHH}-gp130 homodimers (Fig. 11*B*). The EC_{50} of GFP-mCherry–induced proliferation of Ba/F3/gp130/G_{VHH}gp130/C_{VHH}IL-22Rα1 cells was 0.39 ng/ml (Fig. 11*C*). Thus, STAT3 phosphorylation was also specifically induced via G_{VHH}gp130/C_{VHH}IL-22Rα1 heterodimeric receptor complexes induced by GFP-mCherry (Fig. 11*D*). Taken together, gp130 can form biological active receptor complexes with IL-10R2 and IL-22Rα1.

Discussion

Among the switchable synthetic cytokine receptors, the SyCyRs belongs to a new class of fully synthetic cytokine systems featuring combinations of synthetic ligands and synthetic receptors (7). In this study, we present three major findings. First, we show that the SyCyR-principle can be adopted to classes of cytokine receptors other than the IL-6/IL-12 cytokine family. In detail, we generated biologically active synthetic cytokine receptors for IL-22. Our data suggest that replacement of the extracellular domain of cytokine receptors by nanobodies as ligand-binding entities is applicable to a wide range of cytokine receptors with associated tyrosine kinases. Therefore, our findings are in good agreement with other studies, using natural cytokines and chimeric cytokine receptors or so-called synthekines, that receptors with associated kinases can be widely combined irrespective of family membership (11, 30, 31). Second, even though IL-22 signals via a heterodimeric receptor complex consisting of IL-22Rα1 and IL-10R2, we showed that also homodimers of synthetic IL-10R2 but not of IL-22Rα1 are biologically active. Third, SyCyRs for gp130 can form biologically active receptor complexes with synthetic IL-22Rα1 and IL-10R2.

Both receptors for IL-22 belong to the class II cytokine receptor family (32). Long-chain IL-22Rα1 is mainly associated with Jak1, whereas the short-chain IL-10R2 was considered to be mainly associated with Tyk2 (tyrosine kinase 2) (32). The intracellular domain of the long-chain cytokine receptor IL-22Rα1 is 346 amino acid residues long, and apart from predicted box 1 (aa 255–262) and box 2 (aa 282–287) binding sites for Jak1, it also contains a range of canonical activation sites for signal transduction (*e.g.* STATs and ERK1/2) (25). We expected that homodimers of G_{VHH}IL-22Rα1 or C_{VHH}IL-22Rα1 would also induce signal transduction as we have observed this for other homodimeric long-chain receptor chains, including gp130 (2), IL-12Rβ2 (11), and IL-23R (33). Even though homodimers of this synthetic IL-22Rα1 were biologically inactive, this does not necessary mean that an alternative synthetic cytokine receptor composition would also not result in biologically active homodimers. Importantly, the synthetic cytokine receptor for IL-22Rα1 was on the cell surface, and binding of GFP-Fc was verified by flow cytometry. The intracellular domain of the IL-10R2 is, however, only 76 amino acid residues long, and its main function was considered to be the recruitment and activation of Tyk2 (27). So far it has been suggested for the human IL-10R2 that homodimerization can induce phosphorylation of STAT1 (27). However, classical box 1 and box 2 motifs (34) within the intracellular domain of IL-10R2 could not be identified by amino acid sequence comparison. Receptors with short ICDs, including IL-10R2, often bind their ligands with lower affinity, pair with Tyk2 or Jak3, and typically only minimally contribute to STAT recruitment and activation (28, 29). Only in combination with long-chain receptors, such as IL-22Rα1, was IL-10R2 considered to contribute to signal transduction. Indeed, IL-22 initially binds to IL-22Rα1, which increases the affinity for IL-10R2 (35–38). Therefore, it comes as a surprise that homodimers of IL-10R2 induced signal transduction in Ba/F3/gp130/C_{VHH}IL-10R2 cells, including phosphorylation of STAT3 and ERK1/2. Moreover, this was not only triggered by the phosphorylation of Jak1 and Tyk2, which were also

Figure 5. Analysis of IL-10R2 homodimeric signaling using Ba/F3/gp130/C_{VHH}IL-10R2 cells. *A*, schematic illustration of mCherry-Fc homodimer binding two C_{VHH}IL-10R2 receptors. This image was created with BioRender. *B*, proliferation of Ba/F3/gp130/C_{VHH}IL-10R2 cells with increasing concentrations of mCherry-Fc from 0.0001 to 1000 ng/ml. *Error bars*, S.D. ***, $p < 0.001$. One representative experiment, with three biological replicates, of three is shown. *C*, proliferation of Ba/F3/gp130 and Ba/F3/gp130/C_{VHH}IL-10R2 cells incubated without cytokine (−), with 10 ng/ml Hyper-IL-6 or 100 ng/ml mCherry-Fc. For the indicated samples, 10 μM P6 inhibitor was added to the respective cytokine. *Error bars*, S.D. One representative experiment, with four biological replicates, of three is shown. *D*, STAT3, ERK1/2, Jak1, Jak2, and Tyk2 activation in Ba/F3/gp130/C_{VHH}IL-10R2 cells treated with 10 ng/ml Hyper-IL-6 or 100 ng/ml mCherry, mCherry-Fc for 120 min. Cells treated with the P6 inhibitor were preincubated with 10 μM P6 for 30 min and then also stimulated for 120 min. Equal amounts of protein (50 μg/lane) were analyzed via specific antibodies detecting phospho-STAT3, -ERK1/2, -Jak1, -Jak2, and -Tyk2 and STAT3, ERK1/2, Jak1, Jak2, and Tyk2. Western blotting data show one representative experiment of three. *E*, HEK293T cells were co-transfected with cDNAs coding for GFP_{VHH}IL-10R2, GFP_{VHH}IL-10R2 and murine Jak1, GFP_{VHH}IL-10R2 and murine Jak2, or GFP_{VHH}IL-10R2 and murine Tyk2. The kinases were immunoprecipitated by specific antibodies, and Western blotting analysis was performed to detect Myc-tagged GFP_{VHH}IL-10R2. *IP*, coimmunoprecipitation; *L*, lysate. One representative experiment of two is shown.

A

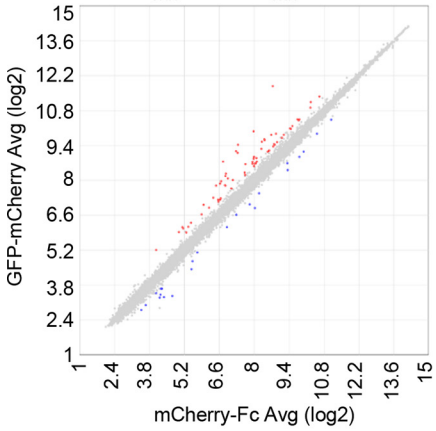

B

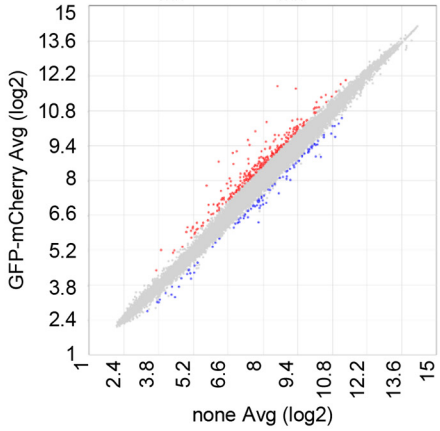

C

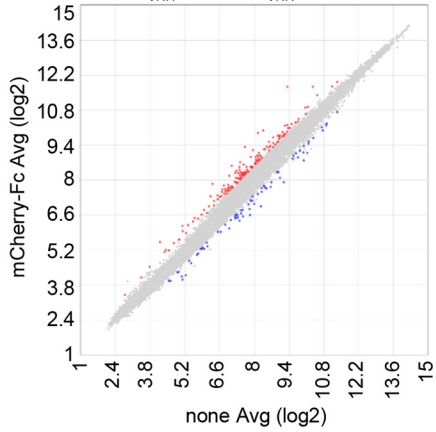

D

GFP-mCherry vs. none		mCherry-Fc vs. none		Gene
Fold change	P-val	Fold change	P-val	
5.14	$1.25*10^{-13}$	5.32	$8.45*10^{-14}$	Pim-1
4.69	$4.18*10^{-12}$	2.04	$3.22*10^{-6}$	Ier3
4.61	$3.00*10^{-15}$	3.37	$2.50*10^{-13}$	Pim-2
3.62	$9.38*10^{-6}$	1.79	0.154	IL-6
2.34	$6.53*10^{-14}$	1.52	$2.88*10^{-8}$	Ifngr2
2.06	$2.11*10^{-12}$	1.93	$1.16*10^{-11}$	Socs3
1.99	$8.43*10^{-15}$	2.63	$1.63*10^{-17}$	Myc
1.89	$1.89*10^{-7}$	2.08	$3.2*10^{-8}$	Gas5
-1.59	0.0004	-1.51	0.0006	Stfa1
-1.53	$1.10*10^{-7}$	-1.51	$3.39*10^{-6}$	Ccng2
-1.55	0.0005	-1.63	$2.84*10^{-5}$	Krtap5-2

E

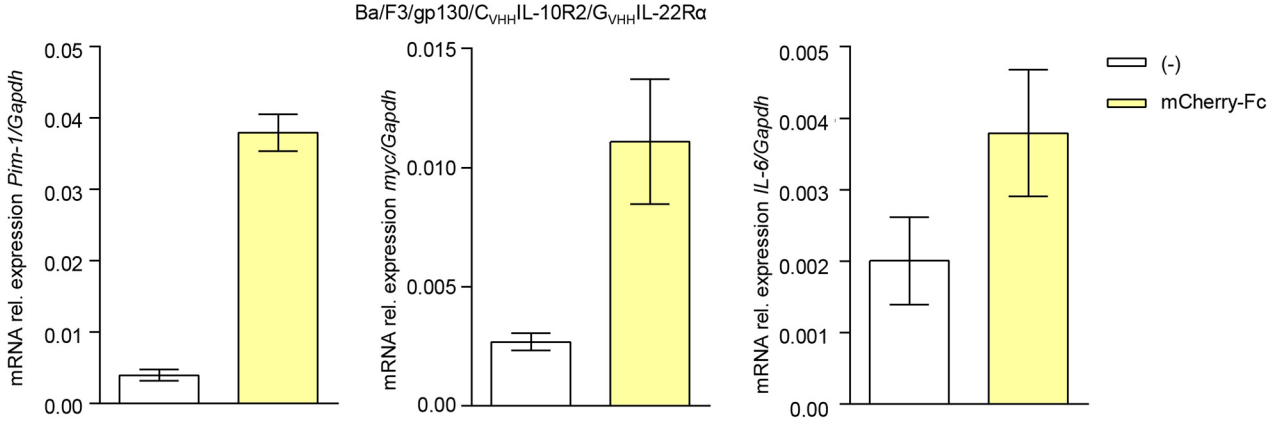

activated by canonical IL-22 signaling but also by Jak2, which we did not observe in natural and synthetic IL-22 signaling. Interaction of Jak2 and G_{VHH}IL-10R2 was verified by co-immunoprecipitation. Based on our homodimeric receptor analysis using deletion variants of C_{VHH}IL-10R2, our results suggest that the amino acid residues from 310 to 330 are responsible for downstream signaling via STATs and ERK1/2. However, we were not able to identify single amino acids that are responsible for STAT and ERK1/2 activation within this 20-amino-acid-residue-long region. A putative P*XX*P motif, which might facilitate binding of SH3 domain proteins such as Grb2 (39, 40), which is involved in activation of the Ras/Raf MAPK pathway, is not involved in STAT and ERK activation as we have shown by introduction of point mutations to exchange proline into alanine, whereas SH2 domains, found in Grb2 but also in STATs, bind to phosphorylated tyrosine-containing peptides (p*YXX*Q motif) (41), which are not present in the IL-10R2. Tyrosine-/SH2-independent STAT activation was reported previously for the granulocyte colony–stimulating factor receptor (G-CSFR; STAT3) (42), IL-22 receptor (IL-22R; STAT3) (43), and interferon-α/β receptor β-chain (IFNAR2; STAT2) (44) and IL-23R (41), and it was speculated that other cytokine receptors may use a similar mode of STAT3 recruitment (44). However, a consensus sequence from these noncanonical STAT activation modi could not be deduced to date. For G-CSFR, STAT3 is not constitutively associated with a tyrosine-mutated G-CSFR (42), and an intermediate molecule might interact with the C-terminal receptor region, which might contain a phosphotyrosine-binding site for the SH2 domain of STAT3 (42). In the case of IL-23R, also STAT3 is not constitutively associated with a short 17-amino-acid-residue-long internal part of the intracellular domain. Dumoutier *et al*. (43) reported that also the C-terminally located 84 amino acid residues of IL-22R allow constitutive association with STAT3, most likely via the coiled-coil domain of STAT3. Mutation of all cytoplasmic tyrosine residues of the IL-22R only partially affects STAT3 activation, and receptor preassociation with STAT3 might assure a faster STAT3 activation in cells with lower endogenous STAT3 expression. SH2-independent recruitment of STAT3 might serve to avoid negative feedback by proteins such as suppressor of cytokine signaling 3 (SOCS3), which can compete with STAT factors for phosphotyrosines (45).

Albeit a slightly reduced Jak phosphorylation was seen for C_{VHH}IL-10R2(Δ310) compared with C_{VHH}IL-10R2(Δ330), only the larger deletion C_{VHH}IL-10R2(Δ280) resulted in complete abrogation of Jak phosphorylation, suggesting that the binding sites of Jak1, Jak2, and Tyk2 are mainly located between amino acid residues 280 and 310. We have previously defined the noncanonical Jak binding sites in the long-chain IL-23R (46), and others have found that a classical proline-rich box 1 motif does not occur in IFNAR1 (47).

Finally, we show that both IL-22 receptors are able to form biologically active receptor complexes with the IL-6 signal-transducing receptor gp130, which appears to be a common feature of interchangeability among cytokine receptors with associated kinases between different receptor families (2).

Whereas IL-10R2 is widely expressed in cells throughout the body, IL-22Rα1 is expressed predominantly in epithelial tissues. In the intestinal epithelium, IL-22 is responsible for immune homeostasis as well as wound healing (18) and plays an important role in the pathogenesis of many intestinal diseases. Therefore, IL-22 is an interesting therapeutic target for many gastrointestinal diseases (48). Our synthetic IL-22 receptor combination might be a useful tool to study the pro- and anti-inflammatory responses in certain cell types. We are aware that the overexpression of cytokine receptors might cause some artifacts in signaling. Therefore, the next step is to use the endogenous promoter by integration of the synthetic receptors in the endogenous gene loci by CRISPR-Cas9 technology. Moreover, transgenic mice with a Cre-inducible SyCyR for IL-22 may allow the cell type–specific dissection of IL-22 function in tissues and disease states. In general, the modular nature of the synthetic GFP and mCherry ligands allows an exact composition of the receptor stoichiometry, to facilitate tailor-made receptor compositions as shown here for IL-22 and IL-6 cross-talk. In general, this technology might also be used to support CAR T-cell therapies by tailor-made synthetic receptors either supporting or suppressing the activity of CAR T cells.

Experimental procedures

Cells and reagents

All cells were grown at 37 °C with 5% CO_2 in a water-saturated atmosphere in Dulbecco's modified Eagle's medium (DMEM) high-glucose culture medium (GIBCO®, Life Technologies, Darmstadt, Germany) with 10% fetal calf serum (GIBCO®, Life Technologies) and 60 mg/liter penicillin and 100 mg/liter streptomycin (Genaxxon Bioscience GmbH, Ulm, Germany). Murine Ba/F3-gp130 cells were obtained from Immunex (Seattle, WA, USA) and grown in the presence of Hyper-IL-6, a fusion protein of IL-6 and soluble IL-6 receptor. 0.2% (10 ng/ml) conditioned medium from a stable clone of CHO-K1 cells secreting Hyper-IL-6 in the supernatant (stock solution ~5 μg/ml as determined by ELISA) was used to maintain Ba/F3-gp130 cells and derivates thereof. The packaging cell line Phoenix-Eco was received from Ursula Klingmüller (DKFZ, Heidelberg, Germany). HEK293T (ACC-635) cells were purchased from the Leibnitz Institute DSMZ-German Collection of Microorganisms and Cell Culture (Braunschweig, Germany). Phospho-STAT3 (Tyr-705; D3A7; catalog no. 9145;

Figure 6. Microarray analysis of Ba/F3/gp130/C_{VHH}IL-10R2/G_{VHH}IL-22Rα1 cells stimulated either with mCherry-Fc as homodimer or with GFP-mCherry as heterodimer. The comparison was performed with 1.5-fold. Varying up-regulated genes are shown in *red* and down-regulated genes in *blue*. *A*, scatter plot comparing mRNA levels of homo- or heterodimeric stimulation of Ba/F3/gp130/C_{VHH}IL-10R2/G_{VHH}IL-22Rα1 cells. Cells were stimulated with 100 ng/ml for 120 min. *B*, scatter plot comparing mRNA levels of Ba/F3/gp130/C_{VHH}IL 10R2/G_{VHH}IL 22Rα1 cells stimulated for 120 min with 100 ng/ml GFP-mCherry or unstimulated. *C*, scatter plot comparing mRNA levels of Ba/F3/gp130/C_{VHH}IL 10R2/G_{VHH}IL 22Rα1 cells either unstimulated or stimulated for 120 min with 100 ng/ml mCherry-Fc. *D*, list of regulated mRNAs for homo- or heterodimeric stimulation with respective -fold change and *p* value. *E*, verification of microarray data by quantification of mRNA expression of three genes (*Pim-1*, *myc*, and *IL-6*) for homo- or heterodimeric stimulation of Ba/F3/gp130/C_{VHH}IL-10R2/G_{VHH}IL-22Rα1 cells. *Error bars*, S.D. One representative experiment, with three biological replicates, of three is shown.

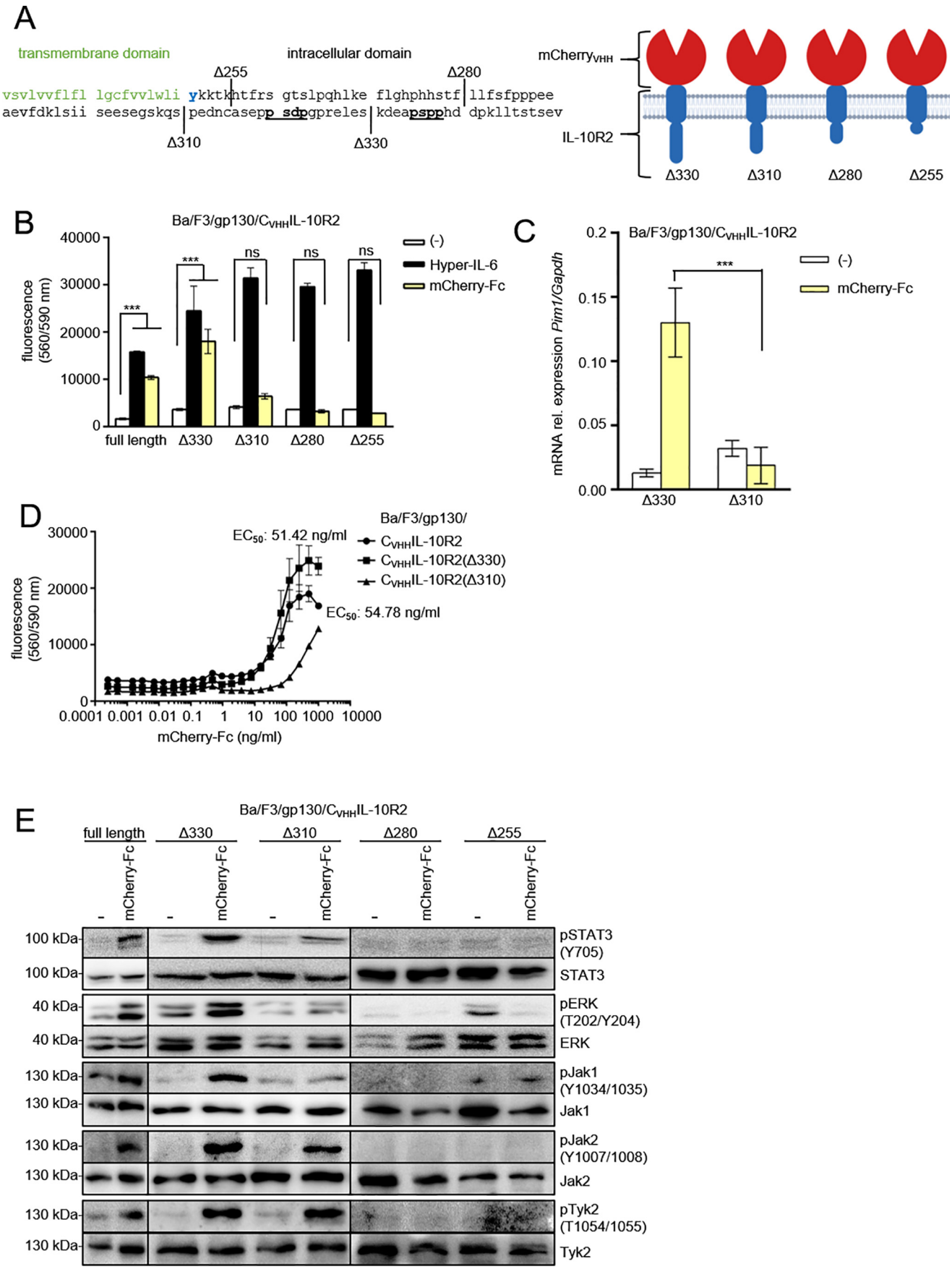
A
transmembrane domain
intracellular domain
Δ255
Δ280
vsvlvvflfl lgcfvvlwli ykktkhtfrs gtslpqhlke flghphhstf llfsfpppee
aevfdklsii seesegskqs pedncasepp sdpgpreles kdeapspphd dpkslltstsev
Δ310
Δ330
mCherry$_{VHH}$
IL-10R2
Δ330
Δ310
Δ280
Δ255
B
Ba/F3/gp130/C$_{VHH}$IL-10R2
fluorescence (560/590 nm)
40000
30000
20000
10000
0
***
***
ns
ns
ns
(-)
Hyper-IL-6
mCherry-Fc
full length
Δ330
Δ310
Δ280
Δ255
C
Ba/F3/gp130/C$_{VHH}$IL-10R2
mRNA rel. expression Pim1/Gapdh
0.2
0.15
0.10
0.05
0.00
***
(-)
mCherry-Fc
Δ330
Δ310
D
Ba/F3/gp130/
EC$_{50}$: 51.42 ng/ml
C$_{VHH}$IL-10R2
C$_{VHH}$IL-10R2(Δ330)
C$_{VHH}$IL-10R2(Δ310)
EC$_{50}$: 54.78 ng/ml
fluorescence (560/590 nm)
30000
20000
10000
0
0.0001 0.001 0.01 0.1 1 10 100 1000 10000
mCherry-Fc (ng/ml)
E
Ba/F3/gp130/C$_{VHH}$IL-10R2
full length
Δ330
Δ310
Δ280
Δ255
-
mCherry-Fc
100 kDa
pSTAT3 (Y705)
STAT3
40 kDa
pERK (T202/Y204)
ERK
130 kDa
pJak1 (Y1034/1035)
Jak1
pJak2 (Y1007/1008)
Jak2
pTyk2 (T1054/1055)
Tyk2

1:1000), STAT3 (124H6; catalog no. 9139; 1:1000), phospho-p44/42 MAPK (ERK1/2; Thr-202/Tyr-204; D13.14.4E; catalog no. 4370; 1:1000), p44/42 MAPK (ERK1/2; catalog no. 9102; 1:1000), phospho-Jak1 (Tyr-1034/1035; catalog no. 3331; 1:1000), Jak1 (6G4; catalog no. 3344; 1:1000), phospho-Jak2 (Tyr-1007/1008; catalog no. 3771; 1:1000), Jak2 (D2E12; catalog no. 3230; 1:1000), phospho-Tyk2 (Tyr-1054/1055; catalog no. 9321; 1:1000), Tyk2 (catalog no. 9312; 1:1000), Myc tag (71D10; catalog no. 2278; 1:1000), and HA tag (C29F4; catalog no. S724S; 1:1000) mAbs were purchased from Cell Signaling Technology (Frankfurt, Germany). The γ-tubulin mAb (catalog no. T5326; 1:5000) was obtained from Sigma–Aldrich (Munich, Germany), and human CIS3/SOCS (C204) mAb (catalog no. JP18391; 1:1000) was supplied by ImmunoBiological Laboratories Co., Ltd. (Fujioka, Japan). Murine IL-10R2 mAb (catalog no. MAB53681; 1:400) was obtained from R&D Systems (Minneapolis, MN, USA). Peroxidase-conjugated secondary mAbs (catalog nos. 31432 and 31462; 1:2500) were obtained from Pierce (Thermo Scientific, St. Leon-Rot, Germany). Alexa Flour 488–conjugated Fab goat anti-rabbit IgG (catalog no. A11070; 1:500) was received from Thermo Fisher Scientific (Waltham, MA, USA). Rat-APC (catalog no. 131724; 1:100) was obtained from Jackson Laboratories (West Grove, PA, USA).

Construction of SyCyRs and synthetic fluorescent ligands

SyCyR pcDNA3.1 expression plasmids were generated by fusion of coding sequence for the IL-11R signal peptide (Q14626, aa 1-22), a Myc tag (EQKLISEEDL; SyCyRs containing GFP_{VHH}), or a FLAG tag (DYKDDDDK) and HA tag (YPYDVPDYA; SyCyRs containing $mCherry_{VHH}$) followed by a nanobody (GFP_{VHH} or $mCherry_{VHH}$), some residues of the extracellular domain (ECD), the complete transmembrane (TMD), and the complete intracellular domain (ICD) of the respective cytokine receptor. For the IL-22Rα-SyCyR, the coding cDNA consists of 10 aa of the ECD and the complete TMD and ICD. The cDNA for the IL-10R2-SyCyR is composed of 10 aa of the ECD and the complete TMD and ICD. The gp130-SyCyR is made up of 13 aa from the ECD and the complete TMD and ICD. Deletion variants of the IL-10R2-SyCyR Δ330, Δ310, Δ280, and Δ255 were generated by amplification of the respective intracellular part via PCR using Phusion® high-fidelity DNA polymerase (Thermo Fisher Scientific). Mutation of the SH3 domain of the IL-10R2 was generated by site-directed mutagenesis using Phusion® high-fidelity DNA polymerase (Thermo Fisher Scientific) followed by DpnI digestion of the methylated template DNA. All SyCyRs were inserted into pMOWS-hygro (49) ($mCherry_{VHH}$) or pMOWS-puro (50) (GFP_{VHH}) vectors for stable transfection of Ba/F3-gp130 cells. All generated plasmids were verified by sequencing.

Generation of synthetic ligands

Synthetic ligands (sequences published previously (2, 5)) were stably expressed in CHO K1 cells using neomycin resistance and single clone selection with 1.125 mg/ml G-418 (Genaxxon Bioscience GmbH). Transfected cells were cultivated with G-418 for 2 weeks, and then single clone selection was carried out with 0.5 cells/well. Single colonies were screened for protein expression. One colony was selected for protein expression in roller bottles (IBS Integra Bioscience, Zizers, Switzerland) with 10% low-IgG fetal calf serum (GIBCO®, Life Technologies) DMEM for 2 months. The supernatant was collected every 3–4 days, and 1 liter of supernatant was used for purification of Fc-tagged proteins using MabSelect^{TM} HiTrap^{TM} columns (GE Healthcare, Chalfront St Giles, UK). Elution was carried out by pH shift using citrate buffer of pH 5.5 and 3.2. Buffer exchange to PBS was achieved using NAP^{TM}-25 columns (GE Healthcare).

Transfection and selection of cells

Ba/F3-gp130 cells were transduced retrovirally using pMOWS plasmids coding for SyCyRs as described previously (41). As the packaging cell line, Phoenix-Eco cells were used. After transduction, cells were grown as described above and supplemented with puromycin (1.5 μg/ml) and/or hygromycin B (1 mg/ml) (Carl Roth, Karlsruhe, Germany).

Cell viability assay

Ba/F3-gp130 cell lines were washed three times with PBS to remove cytokines from the medium. 5×10^4 cells were suspended in DMEM containing 10% fetal calf serum, 60 mg/liter penicillin, and 100 mg/ml streptomycin. Cells were cultured for 3 days in a volume of 100 μl with or without cytokine/synthetic ligands and inhibitors. The CellTiter Blue Viability Assay (Promega, Karlsruhe, Germany) was used to determine the approximate number of viable cells by measuring the fluorescence (excitation 560 nm, emission 590 nm) using the Infinite M200 Pro plate reader (Tecan, Crailsheim, Germany). After adding 20 μl/well of CellTiter Blue reagent (point 0), fluorescence was measured approximately every 20 min for up to 2 h. For each condition of an experiment, 3–4 wells were measured. All values were

Figure 7. Sequential deletion of IL-10R2 intracellular domain and thereby identification of STAT3 binding motif of IL-10R2 homodimer signaling cascade using SyCyR technology. *A*, schematic overview of the transmembrane (*green*) and intracellular domain (*black*) of the IL-10R2. Potential SH3-binding motifs are *underlined*. Deletion variants are marked by Δ*number*. C_{VHH}IL-10R2 deletion variants are shown as an icon with respectively shorter intracellular domains (*blue*). This image was created with BioRender. *B*, proliferation of Ba/F3/gp130/C_{VHH}IL-10R2 (full-length), Ba/F3/gp130/C_{VHH}IL-10R2(Δ330), Ba/F3/gp130/C_{VHH}IL-10R2(Δ310), Ba/F3/gp130/C_{VHH}IL-10R2(Δ280), and Ba/F3/gp130/C_{VHH}IL-10R2(Δ255) cells incubated without cytokine (−), in the presence of 10 ng/ml Hyper-IL-6 or 100 ng/ml mCherry-Fc. *Error bars*, S.D. ***, $p < 0.001$. One representative experiment, with three biological replicates, of three is shown. *C*, quantification of Pim-1 mRNA expression in Ba/F3/gp130/C_{VHH}IL10R2(Δ330) and Ba/F3/gp130/C_{VHH}IL-10R2(Δ310) cells stimulated without cytokine or with 100 ng/ml mCherry-Fc for 120 min. *Error bars*, S.D. ***, $p < 0.001$. One representative experiment, with three biological replicates, of three is shown. *D*, proliferation of Ba/F3/gp130/C_{VHH}IL-10R2, Ba/F3/gp130/C_{VHH}IL-10R2Δ(330), and Ba/F3/gp130/C_{VHH}IL-10R2Δ(310) cells with increasing concentrations of mCherry-Fc from 0.0001 to 1000 ng/ml. *Error bars*, S.D. One representative experiment, with four biological replicates, of four is shown. *E*, STAT3, ERK1/2, Jak1, Jak2, and Tyk2 activation in Ba/F3/gp130/C_{VHH}IL-10R2, Ba/F3/gp130/C_{VHH}IL-10R2(Δ330), Ba/F3/gp130/C_{VHH}IL-10R2(Δ310), Ba/F3/gp130/C_{VHH}IL-10R2(Δ280), and Ba/F3/gp130/C_{VHH}IL-10R2(Δ255) cells treated with 100 ng/ml mCherry-Fc for 120 min. *Vertical lines*, Western blotting *panels* from different experiments. Only protein bands in *lanes* within each demarcated *panel* are comparable. One representative experiment of three is shown.

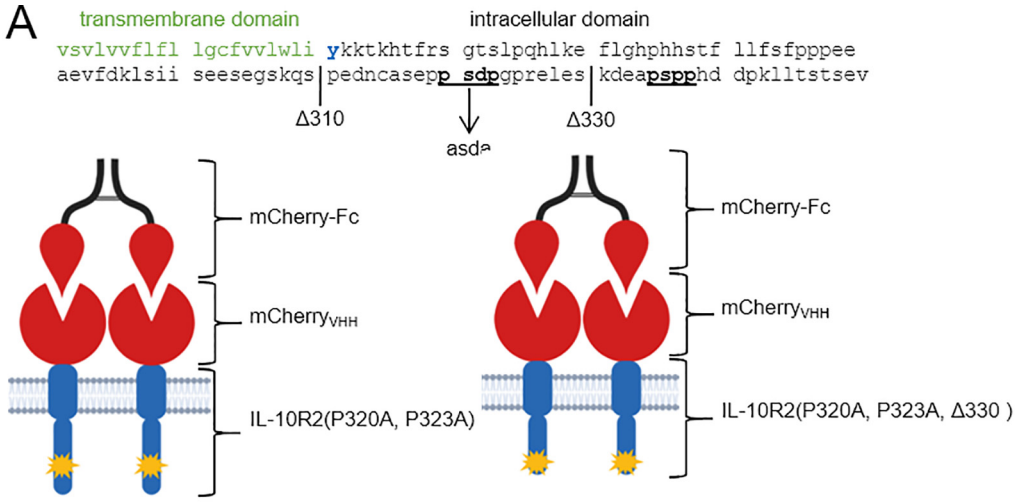
A
transmembrane domain
intracellular domain
vsvlvvflfl lgcfvvlwli ykktkhtfrs gtslpqhlke flghphhstf llfsfpppee
aevfdklsii seesegskqs pedncasepp sdpgpreles kdeapspphd dpkllttstsev
Δ310
asd[a]
Δ330
mCherry-Fc
mCherry$_{VHH}$
IL-10R2(P320A, P323A)
mCherry-Fc
mCherry$_{VHH}$
IL-10R2(P320A, P323A, Δ330)

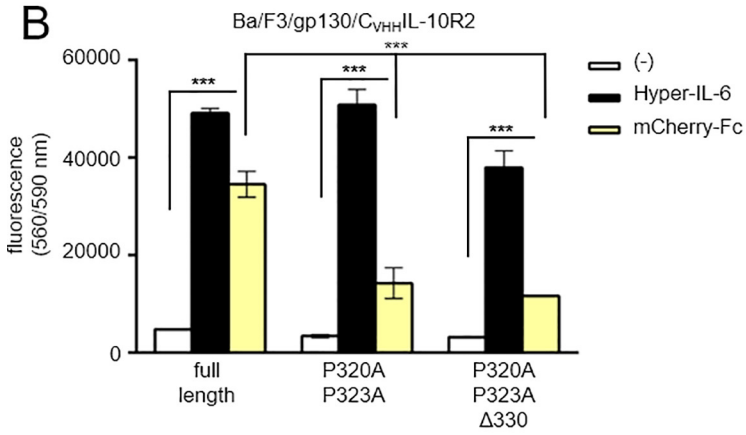
B
Ba/F3/gp130/C$_{VHH}$IL-10R2
fluorescence (560/590 nm)
60000
40000
20000
0
***
***
***
***
(-)
Hyper-IL-6
mCherry-Fc
full length
P320A P323A
P320A P323A Δ330

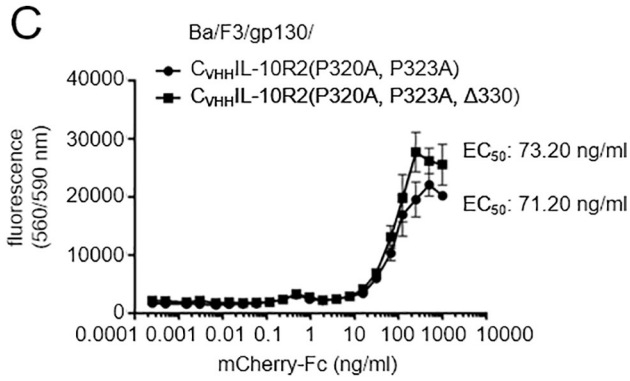
C
Ba/F3/gp130/
C$_{VHH}$IL-10R2(P320A, P323A)
C$_{VHH}$IL-10R2(P320A, P323A, Δ330)
fluorescence (560/590 nm)
40000
30000
20000
10000
0
EC$_{50}$: 73.20 ng/ml
EC$_{50}$: 71.20 ng/ml
0.0001 0.001 0.01 0.1 1 10 100 1000 10000
mCherry-Fc (ng/ml)

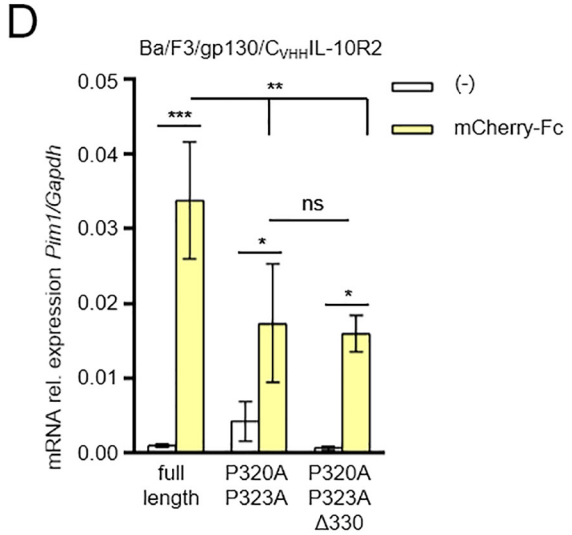
D
Ba/F3/gp130/C$_{VHH}$IL-10R2
mRNA rel. expression Pim1/Gapdh
0.05
0.04
0.03
0.02
0.01
0.00
**
***
ns
*
*
(-)
mCherry-Fc
full length
P320A P323A
P320A P323A Δ330

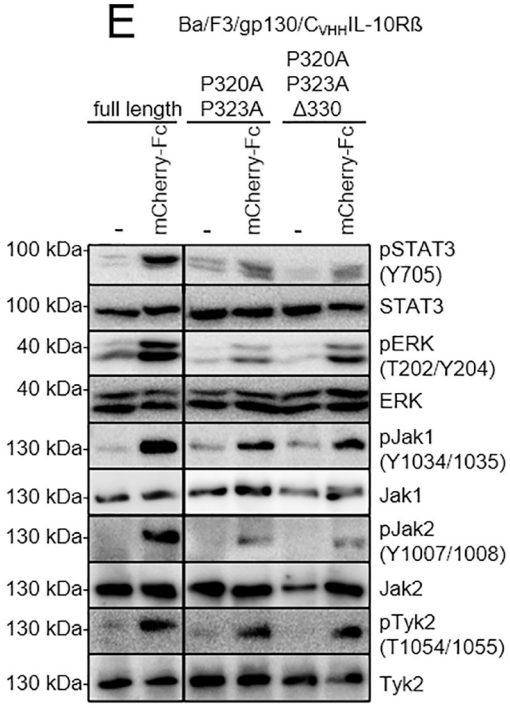
E
Ba/F3/gp130/C$_{VHH}$IL-10Rß
full length
P320A P323A
P320A P323A Δ330
-
mCherry-Fc
100 kDa
pSTAT3 (Y705)
100 kDa
STAT3
40 kDa
pERK (T202/Y204)
40 kDa
ERK
130 kDa
pJak1 (Y1034/1035)
130 kDa
Jak1
130 kDa
pJak2 (Y1007/1008)
130 kDa
Jak2
130 kDa
pTyk2 (T1054/1055)
130 kDa
Tyk2

normalized by subtracting time point 0 values from the final measurement.

Stimulation assay

Ba/F3-gp130 cells were washed four times with PBS to remove cytokines and starved in serum-free DMEM for 4 h. P6 inhibitor was added 30 min prior to stimulation. Cells were stimulated for 1 h (or as indicated if other time points) with 100 ng/ml purified protein, harvested, frozen in liquid nitrogen, and then lysed. Cells were lysed for 1 h with buffer containing 10 mM Tris-HCl, pH 7.8, 150 mM NaCl, 0.5 mM EDTA, 0.5% Nonidet P-40, 1 mM sodium vanadate, 10 mM $MgCl_2$ and a complete, EDTA-free protease inhibitor mixture tablet (Roche Diagnostics, Mannheim, Germany). Protein concentration was determined by a BCA protein assay (Thermo Fisher Scientific) as described by the manufacturer. Protein expression and activation was analyzed as indicated by immunoblotting of 50 μg of each analysis.

Western blotting

50 μg of protein were loaded per lane and separated by SDS-PAGE under reducing conditions and transferred to a polyvinylidene fluoride membrane (Carl Roth). Blotting of membranes was performed with 5% fat-free dried skimmed milk (Carl Roth) in TBS-T (10 mM Tris-HCl pH 7.6, 150 mM NaCl, 0,5% Tween 20) for 4 h. Primary antibodies were diluted in 5% fat-free milk in TBS-T (STAT3, ERK, γ-tubulin) or 5% BSA in TBS-T (pSTAT3, pERK, pJak1, Jak1, pJak2, Jak2, pTyk2, Tyk2, SOCS, HA, Myc) and incubated at 4 °C overnight. Membranes were washed with TBS-T and then incubated with the secondary peroxidase-conjugated antibodies in 5% fat-free dried skim milk in TBS-T for at least 1 h. Signal detection was achieved using the ECL Prime Western blotting detection reagent (GE Healthcare, Freiburg, Germany) and the Chemo Cam Imager (INTAS Science Imaging Instruments, Göttingen, Germany). For a second round of detection, the membranes were stripped with 62.5% Tris-HCl, pH 6.8, 2% SDS, 0.1% β-mercaptoethanol at 60 °C for 30 min and then blocked again in 5% fat-free dried skimmed milk in TBS-T for at least 3 h before using the next primary antibody.

Immunoprecipitation

Immunoprecipitation was performed with HEK293T cells as described (46).

Cell-surface detection of synthetic cytokine receptors

SyCyR expression of stably transfected Ba/F3-gp130 cells was detected by specific antibodies. Cells were washed in FACS buffer (PBS, 1% BSA) and then resuspended in 50 μl of FACS buffer containing the indicated specific primary antibody (Myc 1:100, HA 1:1000). After incubation of at least 1 h at room temperature, cells were washed and then resuspended in 50 μl of FACS buffer containing secondary antibody Alexa Fluor 488–conjugated Fab goat anti-rabbit IgG (catalog no. A11070; 1:500) and incubated for 1 h at room temperature. Cells were washed and resuspended in 500 μl of FACS buffer and analyzed by flow cytometry (BD FACSCanto II flow cytometer, BD Biosciences). Data were evaluated using FlowJo_V10 (FlowJo LLC, Ashland, OR, USA).

Binding of GFP to GFP_{VHH}

The binding of GFP-Fc to the respective GFP_{VHH} was analyzed by flow cytometry using a BD FACSCanto II flow cytometer (BD Biosciences). Cells were incubated without cytokine or with 5 μg/ml GFP-Fc for 1 h at 37 °C with 5% CO_2. Afterward cells were washed three times with PBS, and binding was detected using the FITC-A channel.

Gene expression by real-time PCR

Cells were washed four times with PBS and then starved in serum-free DMEM for 4 h. They were stimulated with 100 ng/ml for 120 min as indicated, harvested, and frozen in liquid nitrogen. RNA isolation was carried out as described above. RNA concentration was determined by a NanoDrop 2000c spectrophotometer (Thermo Scientific, Waltham, MA, USA) and adjusted to 50 ng/μl for all samples. The expression of specific genes was determined by usage of the iTaq™ Universal SYBR Green One-Step Kit (Bio-Rad) as described previously (51). The expression level of *Pim-1* was normalized to the housekeeping gene glyceraldehyde-3-phosphate dehydrogenase (*Gapdh*) for relative quantification and calculated using the $\Delta(Ct_1)$ method.

$$Ratio = \frac{\left(\left(Efficiency_{target} \times 0.01\right)+1\right)^{Ct_{target}}}{\left(\left(Efficiency_{reference} \times 0.01\right)+1\right)^{Ct_{reference}}} \qquad \text{(Eq. 1)}$$

The expression level of target genes was determined by AB17500 Real-Time PCR System (Thermo Scientific, Waltham, MA, USA). The following primer pairs were used in this study: GAPDH, fw 5′ (GAAGGGCTCATGACCACAGT) and rev 5′ (CATTGTCATACCAGGAAATGAGCT); Pim-1, fw 5′

Figure 8. Potential SH3-binding motif of IL-10R2 was mutated, and signal transduction was analyzed. *A*, schematic overview of the transmembrane (*green*) and intracellular domain (*black*) of the IL-10R2. Potential SH3-binding motifs are *underlined*. Deletion variants are marked by Δ*number*. Mutation of the potential SH3-binding motif is indicated with an *arrow*. Prolines 320 and 323 were changed to alanine by mutation of cytosine to guanine. Mutated C_{VHH}IL-10R2 variants are shown as an *icon*: intracellular domains in *blue* and the indicated mutations in *yellow*. This image was created with BioRender. *B*, proliferation of Ba/F3/gp130/C_{VHH}IL-10R2, Ba/F3/gp130/C_{VHH}IL-10R2(P320A,P323A), and Ba/F3/gp130/C_{VHH}IL-10R2(P320A,P323A,Δ330) cells incubated without cytokine (−) and with 10 ng/ml Hyper-IL-6 or 100 ng/ml mCherry-Fc. *Error bars*, S.D. ***, $p < 0.001$. One representative experiment, with three biological replicates, of three is shown. *C*, proliferation of Ba/F3/gp130/C_{VHH}IL-10R2(P320A,P323A) and Ba/F3/gp130/C_{VHH}IL-10R2(P320A,P323A,Δ330) cells with increasing concentrations of mCherry-Fc from 0.0001 to 1000 ng/ml. *Error bars*, S.D. One representative experiment, with four biological replicates, of four is shown. *D*, quantification of Pim-1 expression in Ba/F3/gp130/C_{VHH}IL-10R2 (full-length), Ba/F3/gp130/C_{VHH}IL-10R2(P320A,P323A) and Ba/F3/gp130/C_{VHH}IL-10R2(P320A, P323A,Δ330) cells stimulated with 100 ng/ml mCherry-Fc for 120 min. *Error bars*, S.D. ***, $p < 0.001$; **, $p < 0.01$; *, $p < 0.1$. One representative experiment, with three biological replicates, of three is shown. *E*, STAT3, STAT5, ERK1/2, Jak1, Jak2, and Tyk2 activation in Ba/F3/gp130/C_{VHH}IL-10R2, Ba/F3/gp130/C_{VHH}IL-10R2(P320A,P323A), and Ba/F3/gp130/C_{VHH}IL-10R2(P320A,P323A,Δ330) cells stimulated without cytokine (−) or with 100 ng/ml mCherry-Fc for 120 min. *Vertical lines* indicate different membranes. One representative experiment of three is shown.

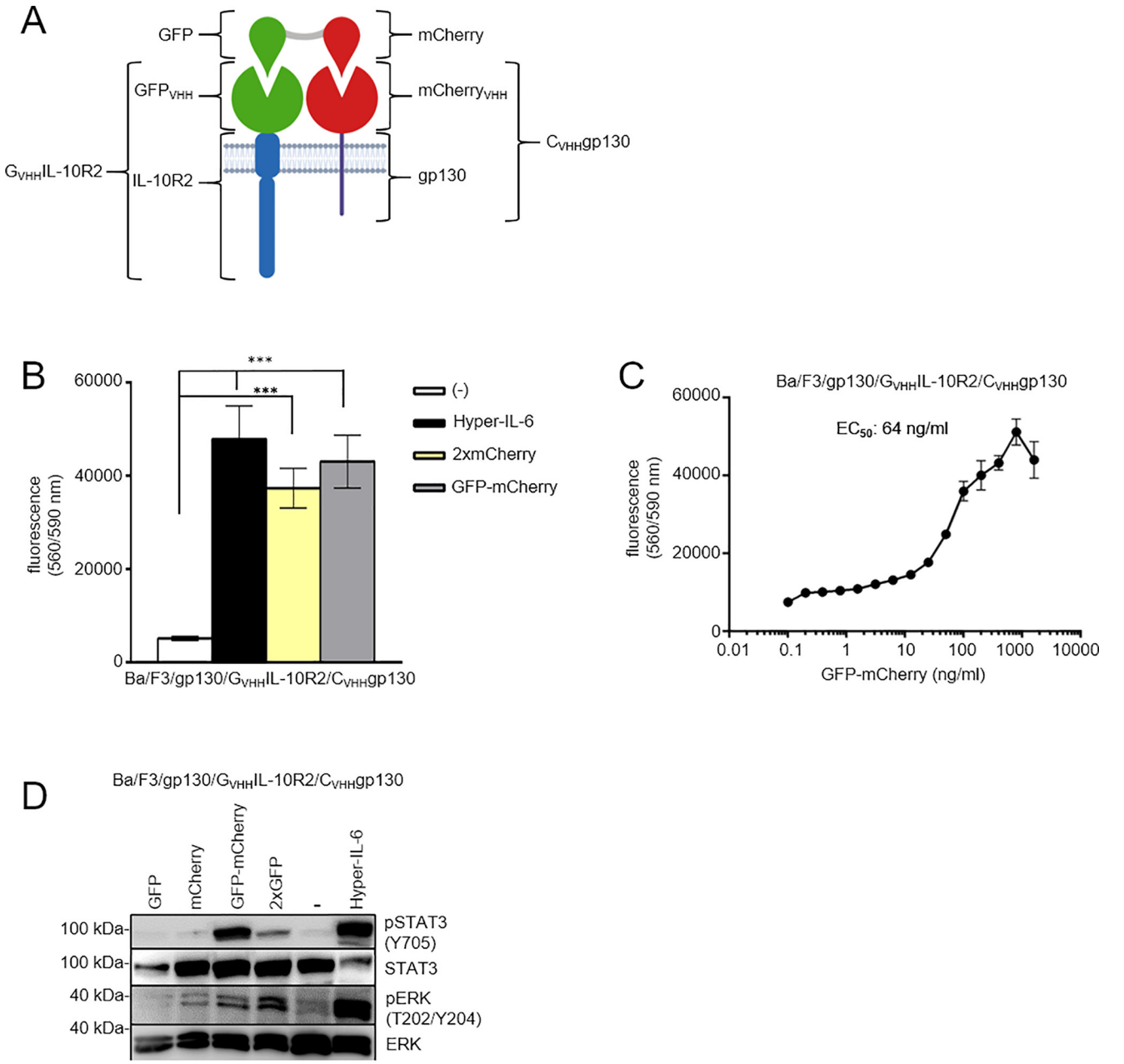

Figure 9. Analysis of new receptor combination IL-10R2 and gp130 using SyCyR technology. *A*, schematic illustration of GFP-mCherry heterodimer binding to G_{VHH}IL-10R2 (*green* and *blue*) and C_{VHH}gp130 (*red* and *purple*) to induce signal transduction. This image was created with BioRender. *B*, proliferation of Ba/F3/gp130/G_{VHH}IL-10R2/C_{VHH}gp130 cells incubated without cytokine (−), with 10 ng/ml Hyper-IL-6 or with 100 ng/ml 2xmCherry, GFP-mCherry. *Error bars*, S.D. ***, $p < 0.001$. One representative experiment, with three biological replicates, of three is shown. *C*, proliferation of Ba/F3/gp130/G_{VHH}IL-10R2/C_{VHH}gp130 cells with increasing concentrations of GFP-mCherry from 0.1 to 2000 ng/ml. *Error bars*, S.D. One representative experiment, with four biological replicates, of three is shown. *D*, STAT3 and ERK1/2 activation of Ba/F3/gp130/G_{VHH}IL-10R2/C_{VHH}gp130 cells treated with 10 ng/ml Hyper-IL-6 or 100 ng/ml GFP, mCherry, GFP-mCherry, or 2xGFP for 60 min. Equal amounts of protein (50 μg/lane) were analyzed by specific antibodies detecting phospho-STAT3 and -ERK1/2 and STAT3 and ERK1/2. One representative experiment of three is shown.

(GATCATCAAGGGCCAAGTGT) and rev 5′ (CCATCTTGGTGACCCAGTCT); c-Myc, fw 5′ (TTCTCAGCCGCTGCCAAGCTGGTC) and rev 5′ (GGTTTGCTGTGGCCTCGGGATGGA); IL-6, fw 5′ (CAAAGCCAGAGTCCTTCAGA) and rev 5′ (GATGGTCTTGGTCCTTAGCC).

Microarray analysis

Ba/F3-gp130-IL-10R2-IL-22-Rα1 and Ba/F3-gp130-mCherry$_{VHH}$-IL-10R2-GFP$_{VHH}$-IL-22Rα1 cells were cultured as described before. Cells were washed four times with PBS to remove cytokines from the medium and then starved for 4 h in serum-free DMEM. Cells were stimulated for 120 min without cytokine or with 100 ng/ml mIL-22, GFP-mCherry, or mCherry-Fc. Total RNA extraction, of four independent biological replicates for the stimulation with IL-22 and six replicates for the stimulation with GFP-mCherry and mCherry-Fc, was carried out by an RNeasy Mini Kit (Qiagen, Hilden, Germany) according to instructions. The microarray analysis was performed as described (2). Data

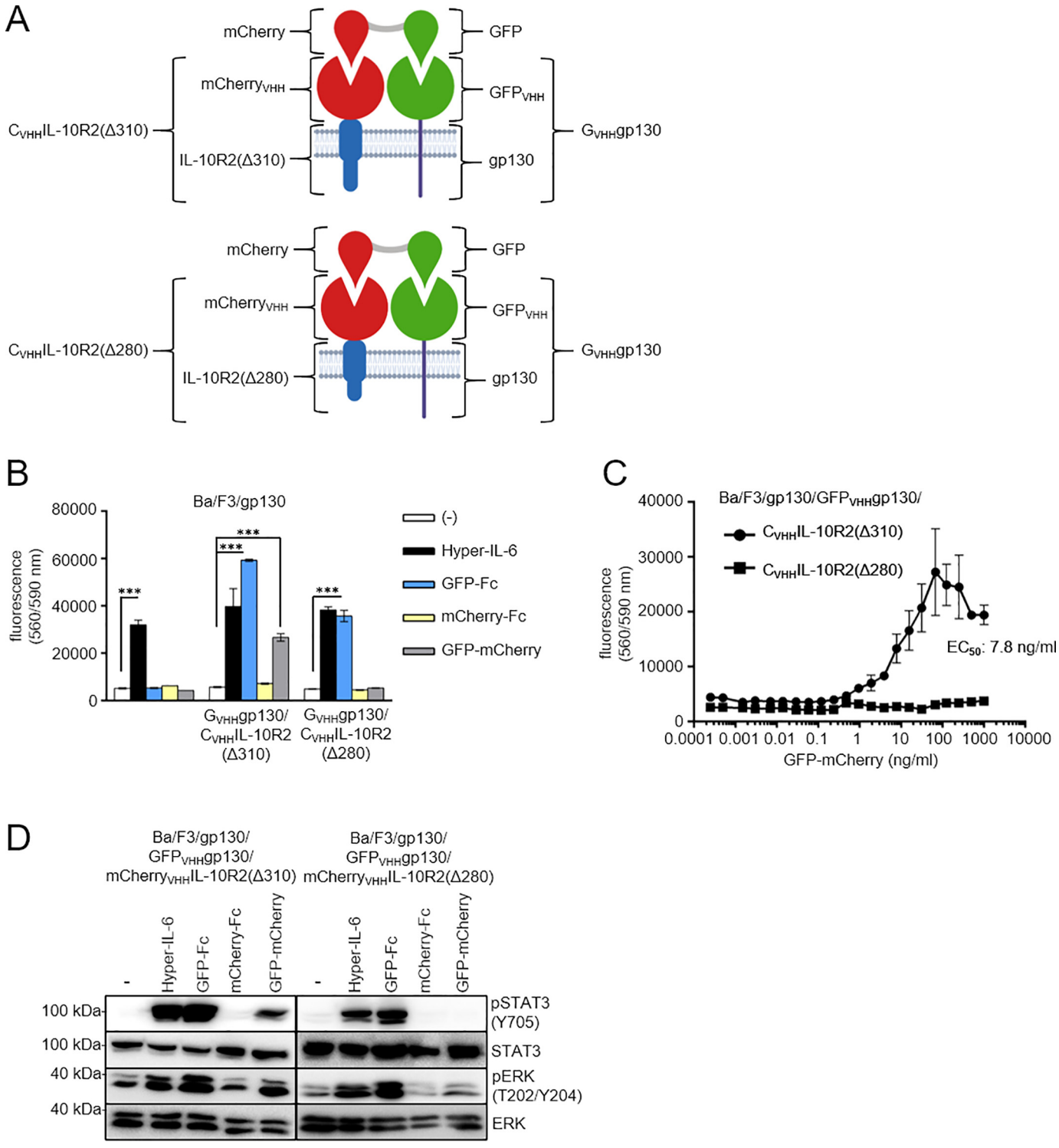

Figure 10. Analysis of new receptor combination using IL-10R2 deletion variants Δ310 and Δ280 in combination with gp130. *A*, schematic illustration of synthetic GFP-mCherry (*red* and *green*) binding to G_{VHH}gp130 (*green* and *purple*) and C_{VHH}IL-10R2 variants Δ310 and Δ280 (*red* and *blue*). This image was created with BioRender. *B*, proliferation of Ba/F3/gp130, Ba/F3/gp130/G_{VHH}gp130/C_{VHH}IL-10R2(Δ310), and Ba/F3/gp130/G_{VHH}gp130/C_{VHH}IL-10R2(Δ280) cells without cytokine (−), in the presence of 10 ng/ml Hyper-IL-6 or in the presence of 100 ng/ml GFP-Fc, mCherry-Fc, or GFP-mCherry. *Error bars*, S.D. ***, $p < 0.001$. One representative experiment, with three biological replicates, of three is shown. *C*, proliferation of Ba/F3/gp130/G_{VHH}gp130/C_{VHH}IL-10R2(Δ310) and Ba/F3/gp130/G_{VHH}gp130/C_{VHH}IL-10R2(Δ280) cells incubated with increasing concentrations of GFP-mCherry from 0.0001 to 1000 ng/ml. *Error bars*, S.D. One representative experiment, with four biological replicates, of three is shown. *D*, STAT3 and ERK1/2 activation in Ba/F3/gp130/G_{VHH}gp130/C_{VHH}IL-10R2(Δ310) and Ba/F3/gp130/G_{VHH}gp130/C_{VHH}IL-10R2(Δ280) cells treated with 10 ng/ml Hyper-IL-6 or 100 ng/ml GFP-Fc, mCherry-Fc, or GFP-mCherry for 120 min. Equal amounts of protein (50 μg/lane) were analyzed via specific antibodies detecting phospho-STAT3 and -ERK1/2 and STAT3 and ERK1/2. *Vertical lines* indicate different membranes. Western blotting data show one representative experiment of three.

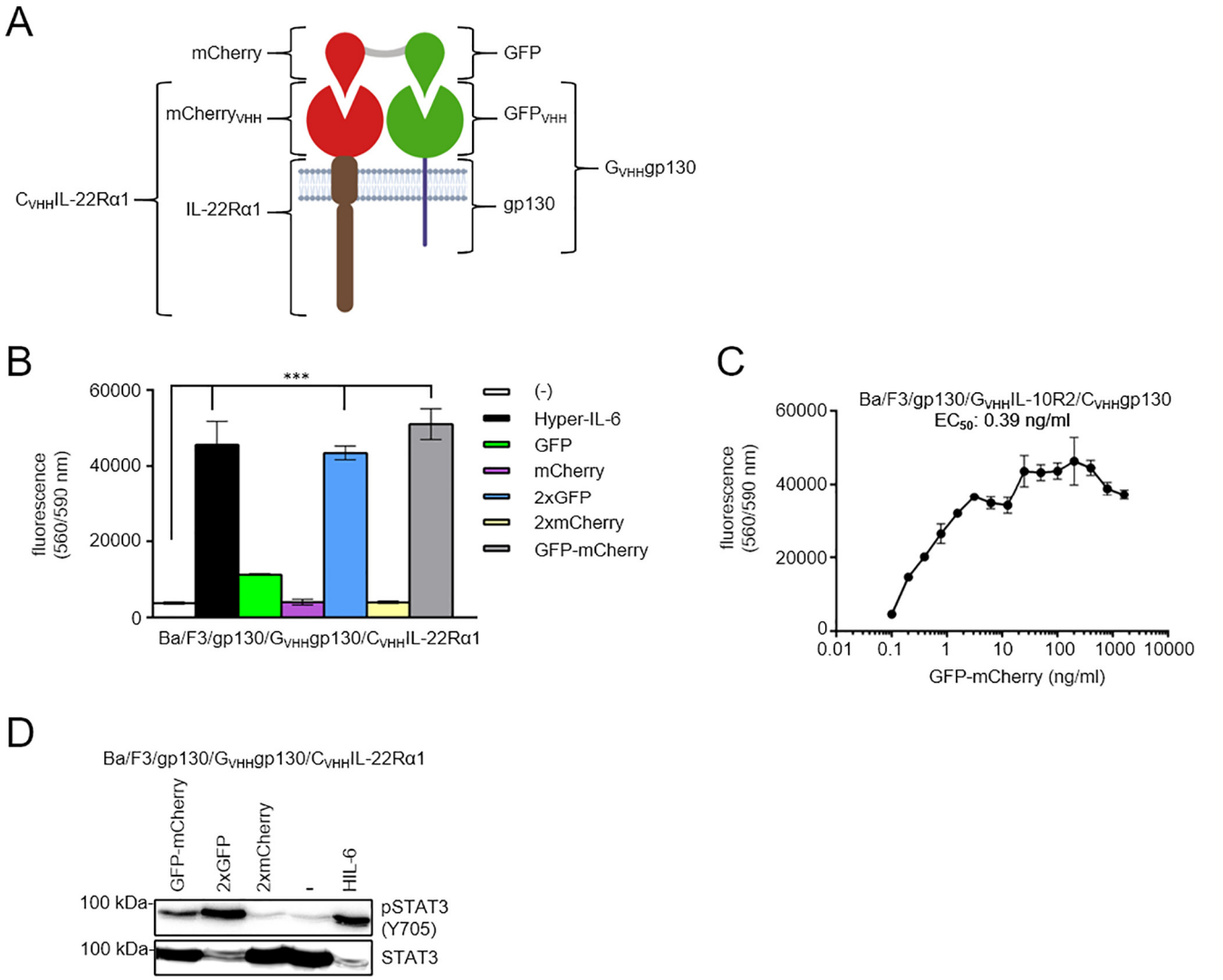

Figure 11. Analysis of cross-talk between the IL-22Rα1 and gp130 SyCyR. *A*, schematic illustration of GFP-mCherry heterodimer binding to C_{VHH}IL-22Rα1 (*red* and *brown*) and G_{VHH}gp130 (*green* and *purple*) SyCyR to induce signal transduction. This image was created with BioRender. *B*, proliferation of Ba/F3/gp130/G_{VHH}gp130/C_{VHH}IL-22Rα1 cells incubated without cytokine (−), with 10 ng/ml Hyper-IL-6 or 100 ng/ml GFP, mCherry, 2xGFP, 2xmCherry, or GFP-mCherry. *Error bars*, S.D. ***, $p < 0.001$. One representative experiment, with three biological replicates, of three is shown. *C*, proliferation of Ba/F3/gp130/G_{VHH}gp130/C_{VHH}IL-22Rα1 cells incubated with increasing concentrations of GFP-mCherry from 0.1 to 2000 ng/ml. *Error bars*, S.D. ***, $p < 0.001$. One representative experiment, with four biological replicates, of three is shown. *D*, STAT3 activation of Ba/F3/gp130/G_{VHH}gp130/C_{VHH}IL-22Rα1 cells treated with 10 ng/ml Hyper-IL-6 or 100 ng/ml 2xGFP, 2xmCherry, or GFP-mCherry. One representative experiment of three is shown.

were analyzed pairwise Ba/F3-gp130-IL-10R2-IL-22-Rα1 cells stimulated with 100 ng/ml IL-22 *versus* without cytokine, Ba/F3-gp130-mCherry$_{VHH}$-IL-10R2-GFP$_{VHH}$-IL-22Rα1 cells stimulated with 100 ng/ml GFP-mCherry *versus* without cytokine, and the same cells stimulated with 100 ng/ml mCherry-Fc *versus* without cytokine. Transcriptome Analysis Console (TAC) software from Thermo Fisher Scientific was used for analysis.

Statistical analysis

Data are shown as mean ± S.D. Multiple comparisons for bar graphs were determined with GraphPad Prism 6 (GraphPad Software, San Diego, CA, USA) using two-way analysis of variance column analyses. Statistical significance was set to $p < 0.05$ (***, $p < 0.001$; **, $p < 0.01$; *, $p < 0.1$).

Data availability

The data of this study are available within the paper. Gene expression raw data have been deposited in the Gene Expression Omnibus (GEO) with the accession number GSE150919.

Acknowledgments—We thank Petra Oprée for assistance.

Author contributions—S. M., M. K., N. F. M., B. K., H. A.-H., and D. M. F. investigation; S. M. and M. K. methodology; S. M., D. M. F., and J. S. writing-original draft; D. M. F. and J. S. conceptualization; J. S. resources; J. S. supervision; J. S. funding acquisition; J. S. validation; J. S. project administration; J. S. writing-review and editing.

Funding and additional information—This work was supported by Deutsche Forschungsgemeinschaft Grants RTG1949 and SFB 1116.

Conflict of interest—The authors declare that they have no conflicts of interest with the contents of this article.

Abbreviations—The abbreviations used are: IL, interleukin; gp130, glycoprotein 130 kDa; IL-22Rα1, interleukin-22 receptor subunit 1; IL-10R2, interleukin-10 receptor 2; STAT, signal transducer and activator of transcription; SOCS, suppressor of cytokine signaling; SyCyR, synthetic cytokine receptor; CAR, chimeric antigen receptor; IFN, interferon; ERK, extracellular signal–regulated kinase; MAPK, mitogen-activated protein kinase; qPCR, quantitative PCR; aa, amino acids; SH2, Src homology 2; SH3, Src homology 3; G-CSFR, granulocyte colony–stimulating factor receptor; DMEM, Dulbecco's modified Eagle's medium; ECD, extracellular domain; TMD, transmembrane domain; ICD, intracellular domain.

References

1. Croxford, A. L., Mair, F., and Becher, B. (2012) IL-23: one cytokine in control of autoimmunity. *Eur. J. Immunol.* **42,** 2263–2273 CrossRef Medline
2. Engelowski, E., Schneider, A., Franke, M., Xu, H., Clemen, R., Lang, A., Baran, P., Binsch, C., Knebel, B., Al-Hasani, H., Moll, J. M., Floë, D. M., Lang, P. A., and Scheller, J. (2018) Synthetic Cytokine Receptors transmit biological signals using artificial ligands. *Nat. Commun.* **9,** 2034 CrossRef Medline
3. Fridy, P. C., Li, Y., Keegan, S., Thompson, M. K., Nudelman, I., Scheid, J. F., Oeffinger, M., Nussenzweig, M. C., Fenyö, D., Chait, B. T., and Rout, M. P. (2014) A robust pipeline for rapid production of versatile nanobody repertoires. *Nat. Methods* **11,** 1253–1260 CrossRef
4. Rothbauer, U., Zolghadr, K., Muyldermans, S., Schepers, A., Cardoso, M. C., and Leonhardt, H. (2008) A versatile nanotrap for biochemical and functional studies with fluorescent fusion proteins. *Mol. Cell. Proteomics* **7,** 282–289 CrossRef Medline
5. Mossner, S., Phan, H., Triller, S., Moll, J., Conrad, U., and Scheller, J. (2020) Multimerization strategies for efficient production and purification of highly active synthetic cytokine receptor ligands. *PLoS ONE* **15,** e0230804 CrossRef Medline
6. Wesolowski, J., Alzogaray, V., Reyelt, J., Unger, M., Juarez, K., Urrutia, M., Cauerhff, A., Danquah, W., Rissiek, B., Scheuplein, F., Schwarz, N., Adriouch, S., Boyer, O., Seman, M., Licea, A., *et al.* (2009) Single domain antibodies: promising experimental and therapeutic tools in infection and immunity. *Med. Microbiol. Immunol.* **198,** 157–174 CrossRef Medline
7. Scheller, J., Engelowski, E., Moll, J., and Floss, D. (2019) Immunoreceptor engineering and synthetic cytokine signaling for therapeutics. *Trends Immunol.* **40,** 258–272 CrossRef Medline
8. Si, W., Li, C., and Wei, P. (2018) Synthetic immunology: T-cell engineering and adoptive immunotherapy. *Synth. Syst. Biotechnol.* **3,** 179–185 CrossRef Medline
9. Collison, L. W., Delgoffe, G. M., Guy, C. S., Vignali, K. M., Chaturvedi, V., Fairweather, D., Satoskar, A. R., Garcia, K. C., Hunter, C. A., Drake, C. G., Murray, P. J., and Vignali, D. A. (2012) The composition and signaling of the IL-35 receptor are unconventional. *Nat. Immunol.* **13,** 290–299 CrossRef Medline
10. Wang, R., Yu, C., Dambuza, I., Mahdi, R., Dolinska, M., Sergeev, Y., Wingfield, P., Kim, S., and Egwuagu, C. (2014) Interleukin-35 induces regulatory B cells that suppress autoimmune disease. *Nat. Med.* **20,** 633–641 CrossRef Medline
11. Floss, D., Schönberg, M., Franke, M., Horstmeier, F., Engelowski, E., Schneider, A., Rosenfeldt, E., and Scheller, J. (2017) IL-6/IL-12 cytokine receptor shuffling of extra- and intracellular domains reveals canonical STAT activation via synthetic IL-35 and IL-39 signaling. *Sci. Rep.* **7,** 15172 CrossRef Medline
12. Ouyang, W., and O'Garra, A. (2019) IL-10 family cytokines IL-10 and IL-22: from basic science to clinical translation. *Immunity* **50,** 871–891 CrossRef Medline
13. Niess, J., Hruz, P., and Kaymak, T. (2018) The interleukin-20 cytokines in intestinal diseases. *Front. Immunol.* **9,** 1373 CrossRef Medline
14. Ouyang, W., Rutz, S., Crellin, N., Valdez, P., and Hymowitz, S. (2011) Regulation and functions of the IL-10 family of cytokines in inflammation and disease. *Annu. Rev. Immunol.* **29,** 71–109 CrossRef Medline
15. Kotenko, S., Izotova, L., Mirochnitchenko, O., Esterova, E., Dickensheets, H., Donnelly, R., and Pestka, S. (2001) Identification of the functional interleukin-22 (IL-22) receptor complex: the IL-10R2 chain (IL-10Rβ) is a common chain of both the IL-10 and IL-22 (IL-10-related T cell-derived inducible factor, IL-TIF) receptor complexes. *J. Biol. Chem.* **276,** 2725–2732 CrossRef Medline
16. Xie, M., Aggarwal, S., Ho, W., Foster, J., Zhang, Z., Stinson, J., Wood, W., Goddard, A., and Gurney, A. (2000) Interleukin (IL)-22, a novel human cytokine that signals through the interferon receptor-related proteins CRF2-4 and IL-22R. *J. Biol. Chem.* **275,** 31335–31339 CrossRef Medline
17. Wolk, K., Kunz, S., Asadullah, K., and Sabat, R. (2002) Cutting edge: immune cells as sources and targets of the IL-10 family members? *J. Immunol.* **168,** 5397–5402 CrossRef Medline
18. Pickert, G., Neufert, C., Leppkes, M., Zheng, Y., Wittkopf, N., Warntjen, M., Lehr, H., Hirth, S., Weigmann, B., Wirtz, S., Ouyang, W., Neurath, M., and Becker, C. (2009) TAT3 links IL-22 signaling in intestinal epithelial cells to mucosal wound healing. *J. Exp. Med.* 1565–1572 CrossRef Medline
19. Dudakov, J., Hanash, A., and van den Brink, M. (2015) Interleukin-22: immunobiology and pathology. *Annu. Rev. Immunol.* **33,** 747–785 CrossRef Medline
20. Negishi, H., Taniguchi, T., and Yanai, H. (2018) The interferon (IFN) class of cytokines and the IFN regulatory factor (IRF) transcription factor family. *Cold Spring Harb. Perspect. Biol.* **10,** a028423 CrossRef
21. Renauld, J. (2003) Class II cytokine receptors and their ligands: key antiviral and inflammatory modulators. *Nat. Rev. Immunol.* **3,** 667–676 CrossRef Medline
22. Schmitz, J., Weissenbach, M., Haan, S., Heinrich, P. C., and Schaper, F. (2000) SOCS3 exerts its inhibitory function on interleukin-6 signal transduction through the SHP2 recruitment site of gp130. *J. Biol. Chem.* **275,** 12848–12856 CrossRef Medline
23. Rajasekhar, K., Madhu, C., and Govindaraju, T. (2016) Natural tripeptide-based inhibitor of multifaceted amyloid β toxicity. *ACS Chem. Neurosci.* **7,** 1300–1310 CrossRef Medline
24. Matsunaga, Y., Inoue, H., Fukuyama, S., Yoshida, H., Moriwaki, A., Matsumoto, T., Matsumoto, K., Asai, Y., Kubo, M., Yoshimura, A., and Nakanishi, Y. (2011) Effects of a Janus kinase inhibitor, pyridone 6, on airway responses in a murine model of asthma. *Biochem. Biophys. Res. Commun.* **404,** 261–267 CrossRef Medline
25. Lejeune, D., Dumoutier, L., Constantinescu, S., Kruijer, W., Schuringa, J., and Renauld, J. (2002) Interleukin-22 (IL-22) activates the JAK/STAT, ERK, JNK, and p38 MAP kinase pathways in a rat hepatoma cell line: pathways that are shared with and distinct from IL-10. *J. Biol. Chem.* **277,** 33676–33682 CrossRef Medline
26. Thompson, J., Cubbon, R., Cummings, R., Wicker, L., Frankshun, R., Cunningham, B., Cameron, P., Meinke, P., Liverton, N., Weng, Y., and DeMartino, J. (2002) Photochemical preparation of a pyridone containing tetracycle: a Jak protein kinase inhibitor. *Bioorg. Med. Chem. Lett.* **12,** 1219–1223 CrossRef Medline
27. Kotenko, S., Izotova, L., Pollack, B., Muthukumaran, G., Paukku, K., Silvennoinen, O., Ihle, J., and Pestka, S. (1996) Other kinases can substitute for Jak2 in signal transduction by interferon-γ. *J. Biol. Chem.* **271,** 17174–17182 CrossRef Medline
28. Murray, P. (2007) The JAK-STAT signaling pathway: input and output integration. *J. Immunol.* **178,** 2623–2629 CrossRef Medline
29. Wang, X., Lupardus, P., Laporte, S., and Garcia, K. (2009) Structural biology of shared cytokine receptors. *Annu. Rev. Immunol.* **27,** 29–60 CrossRef Medline
30. Moraga, I., Spangler, J. B., Mendoza, J. L., Gakovic, M., Wehrman, T. S., Krutzik, P., and Garcia, K. C. (2017) Synthekines are surrogate cytokine and growth factor agonists that compel signaling through non-natural receptor dimers. *Elife* **6,** e22882 CrossRef Medline
31. Zou, J., Presky, D. H., Wu, C. Y., and Gubler, U. (1997) Differential associations between the cytoplasmic regions of the interleukin-12 receptor

subunits β1 and β2 and JAK kinases. *J. Biol. Chem.* **272,** 6073–6077 CrossRef Medline
32. Fickenscher, H., Hör, S., Küpers, H., Knappe, A., Wittmann, S., and Sticht, H. (2002) The interleukin-10 family of cytokines. *Trends Immunol.* **23,** 89–96 CrossRef Medline
33. Hummel, T., Ackfeld, T., Schönberg, M., Ciupka, G., Schulz, F., Oberdoerster, A., Grötzinger, J., Scheller, J., and Floss, D. (2017) Synthetic deletion of the interleukin 23 receptor (IL-23R) stalk region led to autonomous IL-23R homodimerization and activation. *Mol. Cell Biol.* **37,** e00014-17 CrossRef Medline
34. Usacheva, A., Sandoval, R., Domanski, P., Kotenko, S., Nelms, K., Goldsmith, M., and Colamonici, O. (2002) Contribution of the Box 1 and Box 2 motifs of cytokine receptors to Jak1 association and activation. *J. Biol. Chem.* **277,** 48220–48226 CrossRef Medline
35. Yoon, S., Jones, B., Logsdon, N., Harris, B., Deshpande, A., Radaeva, S., Halloran, B., Gao, B., and Walter, M. (2010) Structure and mechanism of receptor sharing by the IL-10R2 common chain. *Structure* **18,** 638–648 CrossRef Medline
36. Logsdon, N., Jones, B., Josephson, K., Cook, J., and Walter, M. (2002) Comparison of interleukin-22 and interleukin-10 soluble receptor complexes. *J. Interferon Cytokine Res.* **22,** 1099–1112 CrossRef Medline
37. Li, J., Tomkinson, K., Tan, X., Wu, P., Yan, G., Spaulding, V., Deng, B., Annis-Freeman, B., Heveron, K., Zollner, R., De Zutter, G., Wright, J., Crawford, T., Liu, W., Jacobs, K., *et al.* (2004) Temporal associations between interleukin 22 and the extracellular domains of IL-22R and IL-10R2. *Int. Immunopharmacol.* **4,** 693–708 CrossRef Medline
38. Jones, B., Logsdon, N., and Walter, M. (2008) Structure of IL-22 bound to its high-affinity IL-22R1 chain. *Structure* **16,** 1333–1344 CrossRef Medline
39. Kay, B., Williamson, M., and Sudol, M. (2000) The importance of being proline: the interaction of proline-rich motifs in signaling proteins with their cognate domains. *FASEB J.* **14,** 231–241 CrossRef Medline
40. Mayer, B. (2001) SH3 domains: complexity in moderation. *J. Cell Sci.* **114,** 1253–1263 Medline
41. Floss, D. M., Mrotzek, S., Klöcker, T., Schröder, J., Grötzinger, J., Rose-John, S., and Scheller, J. (2013) Identification of canonical tyrosine-dependent and non-canonical tyrosine-independent STAT3 activation sites in the intracellular domain of the interleukin 23 receptor. *J. Biol. Chem.* **288,** 19386–19400 CrossRef Medline
42. Ward, A., Hermans, M., Smith, L., van Aesch, Y., Schelen, A., Antonissen, C., and Touw, I. (1999) Tyrosine-dependent and -independent mechanisms of STAT3 activation by the human granulocyte colony-stimulating factor (G-CSF) receptor are differentially utilized depending on G-CSF concentration. *Blood* **93,** 113–124 CrossRef Medline
43. Dumoutier, L., de Meester, C., Tavernier, J., and Renauld, J. (2009) New activation modus of STAT3: a tyrosine-less region of the interleukin-22 receptor recruits STAT3 by interacting with its coiled-coil domain. *J. Biol. Chem.* **284,** 26377–26384 CrossRef Medline
44. Li, X., Leung, S., Kerr, I., and Stark, G. (1997) Functional subdomains of STAT2 required for preassociation with the α interferon receptor and for signaling. *Mol. Cell Biol.* **17,** 2048–2056 CrossRef Medline
45. Palmer, D., and Restifo, N. (2009) Suppressors of cytokine signaling (SOCS) in T cell differentiation, maturation, and function. *Trends Immunol.* **30,** 592–602 CrossRef Medline
46. Floss, D., Klöcker, T., Schröder, J., Lamertz, L., Mrotzek, S., Strobl, B., Hermanns, H., and Scheller, J. (2016) Defining the functional binding sites of interleukin 12 receptor β1 and interleukin 23 receptor to Janus kinases. *Mol. Biol. Cell* **27,** 2301–2316 CrossRef Medline
47. Wallweber, H., Tam, C., Franke, Y., Starovasnik, M., and Lupardus, P. (2014) Structural basis of recognition of interferon-α receptor by tyrosine kinase 2. *Nat. Struct. Mol. Biol.* **21,** 443–448 CrossRef Medline
48. Parks, O., Pociask, D., Hodzic, Z., Kolls, J., and Good, M. (2015) Interleukin-22 signaling in the regulation of intestinal health and disease. *Front. Cell Dev. Biol.* **3,** 85 CrossRef Medline
49. Suthaus, J., Tillmann, A., Lorenzen, I., Bulanova, E., Rose-John, S., and Scheller, J. (2010) Forced homo- and heterodimerization of all gp130-type receptor complexes leads to constitutive ligand-independent signaling and cytokine-independent growth. *Mol. Biol. Cell* **21,** 2797–2807 CrossRef Medline
50. Ketteler, R., Moghraby, C., Hsiao, J., Sandra, O., Lodish, H., and Klingmüller, U. (2003) The cytokine-inducible Scr homology domain-containing protein negatively regulates signaling by promoting apoptosis in erythroid progenitor cells. *J. Biol. Chem.* **278,** 2654–2660 CrossRef Medline
51. Fazel Modares, N., Polz, R., Haghighi, F., Lamertz, L., Behnke, K., Zhuang, Y., Kordes, C., Häussinger, D., Sorg, U., Pfeffer, K., Floss, D., Moll, J., Piekorz, R., Ahmadian, M., Lang, P., *et al.* (2019) IL-6 trans-signaling controls liver regeneration after partial hepatectomy. *Hepatology* **70,** 2075–2091 CrossRef Medline